IOWA STATE UNIVERSITY
Digital Repository

Retrospective Theses and Dissertations

2008

Force and moment analysis of stacked counter rotating eccentric mass tree shaker energy-wheel system

Lloyd Dale Snell
Iowa State University

Follow this and additional works at: http://lib.dr.iastate.edu/rtd

 Part of the Agriculture Commons, and the Bioresource and Agricultural Engineering Commons

Recommended Citation
Snell, Lloyd Dale, "Force and moment analysis of stacked counter rotating eccentric mass tree shaker energy-wheel system" (2008). *Retrospective Theses and Dissertations*. 15403.
http://lib.dr.iastate.edu/rtd/15403

This Thesis is brought to you for free and open access by Iowa State University Digital Repository. It has been accepted for inclusion in Retrospective Theses and Dissertations by an authorized administrator of Iowa State University Digital Repository. For more information, please contact digirep@iastate.edu.

Force and moment analysis of stacked counter rotating eccentric mass tree shaker energy-wheel system

by

Lloyd Dale Snell

A thesis submitted to the graduate faculty

in partial fulfillment of the requirements for the degree of

MASTER OF SCIENCE

Major: Agricultural Engineering

Program of Study Committee:
Stuart J. Birrell, Major Professor
Steven Mickelson
Brian Steward

Iowa State University

Ames, Iowa

2008

Copyright © Lloyd Dale Snell, 2008. All rights reserved

UMI Number: 1454712

Copyright 2008 by
Snell, Lloyd Dale

All rights reserved

INFORMATION TO USERS

The quality of this reproduction is dependent upon the quality of the copy submitted. Broken or indistinct print, colored or poor quality illustrations and photographs, print bleed-through, substandard margins, and improper alignment can adversely affect reproduction.

In the unlikely event that the author did not send a complete manuscript and there are missing pages, these will be noted. Also, if unauthorized copyright material had to be removed, a note will indicate the deletion.

UMI®

UMI Microform 1454712
Copyright 2008 by ProQuest LLC
All rights reserved. This microform edition is protected against unauthorized copying under Title 17, United States Code.

ProQuest LLC
789 East Eisenhower Parkway
P.O. Box 1346
Ann Arbor, MI 48106-1346

TABLE OF CONTENTS

LIST OF FIGURES

LIST OF TABLES

ABSTRACT

The tree shaker is a high throughput hydro-mechanical systems used in nut and fruit harvest. Many commercial tree shakers use stacked counter rotating eccentric mass energy-wheels to dislodge the crop from the tree by attaching and shaking the trunk. Tree shakers are known to cause tree trunk damage by approach impact, barking, and bruising of the tree trunk. Tree trunk damage, catastrophic or accumulative, could account for a 4% lifetime production loss, 1408 kg/hectare.

The energy-wheels are commonly known to create planer pulse forces. The pulse is created by the rotation of eccentric mass about a fixed common shaft. The frequency and magnitude of the force is determined by the weight, angular velocity, and center of gravity location of each energy wheel. The industry has developed pads and slings to conform to the tree trunk and transmit the force while minimizing the potential for trunk damage. Lubrication of the slings reduces the coefficient of friction and allows unwanted force dissipation. Lubrication of the slings reduce the transfer of non-normal forces.

This research discloses the presence of moments and extends the planer equations to allow analysis of moment magnitudes and the introduction of planer losses in the y-axis. Moments and planer forces are always present in stacked counter rotating eccentric mass energy-wheel systems. Moments are non-normal forces and are dissipated in the slings, pads, shaker head suspension system. Moments and y-axis losses reduce the efficiency of the system and require additional hardware and systems to control adverse effects on the tree trunk.

Understanding the magnitude of moments will allow development of new systems to extend the application of mechanical shakers to other crops and applications.

CHAPTER 1. INTRODUCTION

Figure 1. OMC Shaker clamped to the trunk of an almond tree.

In the hot dry heat of late summer, a tree shaker positioned below the dusty green tree canopies of an almond orchard in the Central Valley of California prowls toward a tree (Figure 1). It is guided quickly to a stop by the operator, its shaker head positioned around the tree. The clamp cylinder is energized, compressing and conforming pads around the trunk while subtly twisting the shaker head and tree trunk into an uncomfortable alignment. The hydraulic system then automatically sequences from the clamping circuit to the shaking circuit, launching the shaker head into a vigorous shaking pattern for approximately three seconds. The crop rains down in a cloud of dust and debris, unburdening the tree branches and allowing them to spring in relief toward the sky. During these three seconds, the soil cracks at the base of the tree, resonating the vibration through the orchard floor. When the shake lever is released, the hydraulic system screeches under dynamic braking and the shaker head brakes hard to a stop. The shaker head is then unclamped, and the engine roars to maximum speed, accelerating the clamp arm open. The tree shaker accelerates away from the tree and the harvest of the tree is complete. This process is then repeated every 15-30 seconds depending on the crop, tree spacing, planting pattern, shaker type, and operator.

The modern tree shaker harvests a diversity of crops including almonds, walnuts, pecans, pistachios, and cherries. The United States Department of Agriculture (United State Department of

Agriculture, 2007) reports that the value of mechanically shaken crops harvested annually is $3.95 billion (Table 1) and the calculated number of trees shaken in the process is 95 million (Table 2).

Table 1. Bearing acres and value of crops harvested by mechanical tree shaking (after United States Department of Agriculture, 2007)

United States - 2007 Crop Statistics

Crop	Bearing Acreage	Yield per hectare	Production	Price per kg	Value
	1000 hectare	*kg*	*1,000 kg*	*Dollars*	*1,000 dollars*
Almonds[1] (in-shell)	235	4,416	1,100,000	3.48	2,127,375
Walnuts (in-shell)	85	3,346	295,000	2.56	754,000
Pistachios (in-shell)	42	4,120	189,000	2.98	561,600
Pecans (in-shell)	94[3]	1,872[2]	175,000	2.49	434,725
Cherries	14	8,182	113,000	0.60	67,923
Totals	370		1,872,000		3,945,623

[1] Yield based on in-shell basis. Shelling ratio for 2007 is 0.573.
[2] Based on data from Historical Background of Pecan Plantings in the Western Region, (Herrera, 2000).
[3] Calculated: Bearing Acreage = Production / Yield per hectare.

Table 2. Typical tree density per hectare and total tree shaken per year

United States - Tree density and number of trees shaken per year

Crop	Trees per hectare			Trees shaken[6]
	Min.	*Max*	*Average*	*Total*
Almonds[1]	185	299	242	56,840,000
Walnuts[2]	79	292	185	16,125,000
Pistachios[3]	272	358	316	13,387,500
Pecans[4]	25	74	49	4,615,569
Cherries[5]	247	383	316	4,424,250
Totals				95,392,319[6]

[1] (Freeman, Viveros, Klonsky, & De Moura, 2008)
[2] (Walnut Marketing Board, 2008)
[3] (Mosz, 2002)
[4] (Bell, 2001)
[5] (Moser Fruit Tree Sales, Inc.)
[6] Tree shaken = production hectare (Table 1) / Average trees per hectare

The mechanical tree-shaker, as seen in Figure 1; is a hydro-mechanical system that has evolved into a reliable and invaluable harvesting technology since the 1960s. Without the utilization of mechanical harvesting, the successful large-scale cultivation of many nut and fruit crops would be economically infeasible. The advantages of mechanical tree shakers include minimized labor cost, high crop removal, crop flexibility, and high throughput. The disadvantages of mechanical tree shakers include trunk or limb damage, water stress, and root zone disruption. Trunk and limb damage are caused by the interaction of the mechanical tree shaker and the tree's biology. Trunk or limb damage at the clamp zone is one of the most common causes of orchard asset losses due to mechanical shaking. This damage is defined as "barking," and is shown in Figure 2. Barking can be either an open tear or bruising at the cambium layer which damages the xylem and phloem cells responsible for nutrient transfer. To reduce such damage, pre-harvest cultural practices induce water stress by shutting off irrigation. Water stress causes the moisture in the tree to be drawn down from the xylem and phloem cells, forcing the bark to draw up tight around the tree. When the bark is tight and dry, there is less chance of barking.

Figure 2. Tree trunk damage, barking, due to shaker head impact with the tree.

However, during the harvesting process operator error due to excessive speed, fatigue, or lack of training, can impact the shaker head with the tree trunk which is a primary cause of an open wound. An open wound requires immediate attention to prevent the loss of a tree asset. If unattended, the wound becomes the entrance point for disease, a barrier for nutrition flow, a source of canker development, and the cause of a redirection of energy that would otherwise be used for crop production in subsequent years. Barking also includes less visible damage resembling bruising rather than an open wound. A severely bruised trunk will feel soft to the touch with a definite separation from the trunk. Milder damage also includes discoloration of the bark after shaking. Bruising also diverts crop production energy toward healing and survival. Trunk damage is most often caused by the use of excessive or insufficient clamping force, improper clamp angle adjustment, insufficient irrigation cut-off time, worn shaker hardware, insufficient pad lubrication, improper pads, and operator inexperience. To reduce operator error, recent efforts have focused on introducing computer control of the shaker head extension, auto clamping and shake sequence (Mayo, 2002).

Tree shaking can also result in cumulative damage due to repeated localized biological damage resulting from clamping and force transfer during the shaking process. Growers have developed cultural practices that alternate the clamping direction each time a shaking operation is performed, to minimize this localized damage. Cumulative damage is hard to measure on a year-to-year basis, as crop yields are affected by weather, pests, fertilizer, pruning, pollination, and many other cultural practices. Often, the existence of long-term damage is evident only when the tree or limb is no longer productive.

Many scientific studies and patents have searched for solutions to minimize production losses due to tree damage at the clamping zone (Compton, 1990a; Ferrari and Evans, 2002; McCrill, 1992; Hill, 1997; Blue Diamond Growers, 2008). The main challenges at the clamping zone are conforming the pads firmly around irregular trunk shapes, firmly gripping during shaking, and discharging excessive heat that builds up during the shaking process. If not dispersed, intense heat can cause pads

and slings to degrade, locally abrade, or split. In the early shaker designs, intense heat could even cause the hollow shell-filled pillow pads to explode. Most of these adverse effects have been mitigated by improvements in design of the shaker slings, pads, and lubrication systems, materials, and shaking processes.

Early shaker heads and transportation systems were also susceptible to high cycle fatigue failures. Shaker head evolution over time included, the utilization of thicker sections, higher strength materials, and localized structural improvements to counter the destructive effects on tree shakers. Improvements resulted in more robust and reliable shaker heads, which were larger and heavier with each production generation. With the additional mass of the shaker head structure, the hydro-mechanical stacked eccentric mass energy-wheels, which is the most successful low-cost vibration system, also became larger to provide greater dynamic forces to overcome the greater inertia forces of the shaker head and tree. This forced increases in both the hydraulic and engine power requirements. In the end, this increase in size to prevent high cycle fatigue required the pad and slings to dissipate even more heat. The new structure in one area, often only transferred the structural failure to another location and the cycle of larger and more robust shaker heads continued.

Mechanical tree harvesting processes can and do cause direct, and indirect damage to the tree. Indirect damage is the stress occurred when the orchard is water stressed prior to harvest in order to prevent trunk damage during shaking. Direct damage is damage caused by the shaker during any phase of the tree shaking process. This damage often results in production losses due to nutrition disruption to a limb or tree death. Almond orchards are capital intensive and take five years to enter economical production. Generally, the prime productive life is approximately 20-25 years (Almond Board of California, 2008) and any damage that leads to tree damage or loss in the final 5-8 years is rarely replaced. The success of replanting trees is also limited by different cultural requirements of new versus established trees, such as competition for light. Mature trees expand into voided areas, increase in production, while new trees will be shaded more, and thus develop more slowly.

With such industry focus on the preventing of tree damage, how significant is the production loss if 1% tree damage due to mechanical shaking is acceptable. The 1% tree damage per year was determined as a starting point based on personnel experience, and discussions with farmers like Don Davis, Manager of Alina Farms in McFarland, California, (Davis, 2008). In these discussions the question, "Is one tree in a hundred damaged by the tree shaker?" or, "Do two or more trees in a hundred have partial damage sufficient enough to equal 1% damage due to tree shaking?" The answer is probably. The industry has an understanding that shaking can be damaging. In fact, tree shaking in the almond industry can be very damaging if the mechanical quality of the equipment and the operator skill are not sufficient to prevent damage. Currently, no data identifies tree shaker damage, type, and magnitude, for seasonal or long-term cumulative damage. The magnitude of loss due to mechanical tree shaking was estimated using a Monte Carlo simulation using the following constraints.

1. Third and fourth leaf production are not included.
2. Full production of an almond tree begins at fifth leaf.
3. Total productive life of the orchard is 25 years.
4. A 1%.probability of tree damaged is assumed per shaking event.
5. The model assumes only a single shaking event per year. This shaking event is for the removal of the crop.
6. A damaged tree is assumed as a 100% loss. No weighting is applied to account for barking or bruising as the cause of production loss.
7. Lost trees are replanted and are not shaken or used in production calculations until the fifth leaf.
8. Assumptions are for almond tree production was developed using the historical production mean and standard deviation production, kg/hectare (Almond Board of

California, 2007). These values were divided by the trees/hectare to develop a normal distribution for individual tree production.

Table 3. Almond Board of California historical data of almond production, kg/hectare (Almond Board of California, 2007).

Year	Almond Production, kg/hectare	Year	Almond Production, kg/hectare
1987	1771	1997	1927
1988	1580	1998	1266
1989	1334	1999	1927
1990	1804	2000	1546
1991	1356	2001	1759
1992	1535	2002	2241
1993	1334	2003	2118
1994	1905	2004	1972
1995	992	2005	1771
1996	1334	2006	2140

Average, trees/hectare	242
Average, production/hectare	1681
StDev, production/hectare	338
Average, production/tree	6.94
StDev, production/tree	1.40

9. Crystal Ball Software[i] was utilized to statistically simulate the theoretical effects of shaker damage over the life of an orchard, Appendix 1.
10. Two hundred and forty two trees are used as the average planting density (Table 2). This simulation has a column for each tree. Each tree is check each for:
    a. Age, is the age of the tree based on the previous year. If the tree is damage in the orchard lifetime the age of the tree is reset to zero the following year the damage event. It often takes a year to define the damaged tree, remove, and prepare to replant a new tree.

b. Damage logic, is a random distribution were zero is no damage and one is damage. Damage can only occur if the tree is greater than or equal to five years old.
c. Harvest logic, set the variable to one if the tree is greater than or equal to five years old and zero otherwise.
d. Gross harvest, is the value randomly generated from a normal distribution using the production data mean and standard deviation per tree (Table 3).
e. Net harvest, is gross harvest multiplied by harvest logic to determine the trees annual production.
f. Gross annual production is the sum of the gross harvest values.
g. Gross net annual production is the sum of the tree net harvest values.
h. Gross orchard production is the sum of gross annual production.
i. Gross net production is the sum of the gross net annual production.

11. Number of trials is set to 5000.

The Monte Carlo simulation show that 1% shaker damage results 1408 kg/hectare lifetime production loss based on a 95% confidence interval (Figure 3). When compared to the lifetime production without loss, damage due to tree shaking results in a lifetime production loss of 4% (Figure 4). If the cost due to mechanical harvest could be eliminated the gross value of delivered product would increase annually $85 million. If a reduction in tree damage (0.5%) along with extending the lifetime production by one year (26 years) an orchard would yield a 107% (2324 kg/hectare) over an orchard with the 1% damage rate (Figure 5).

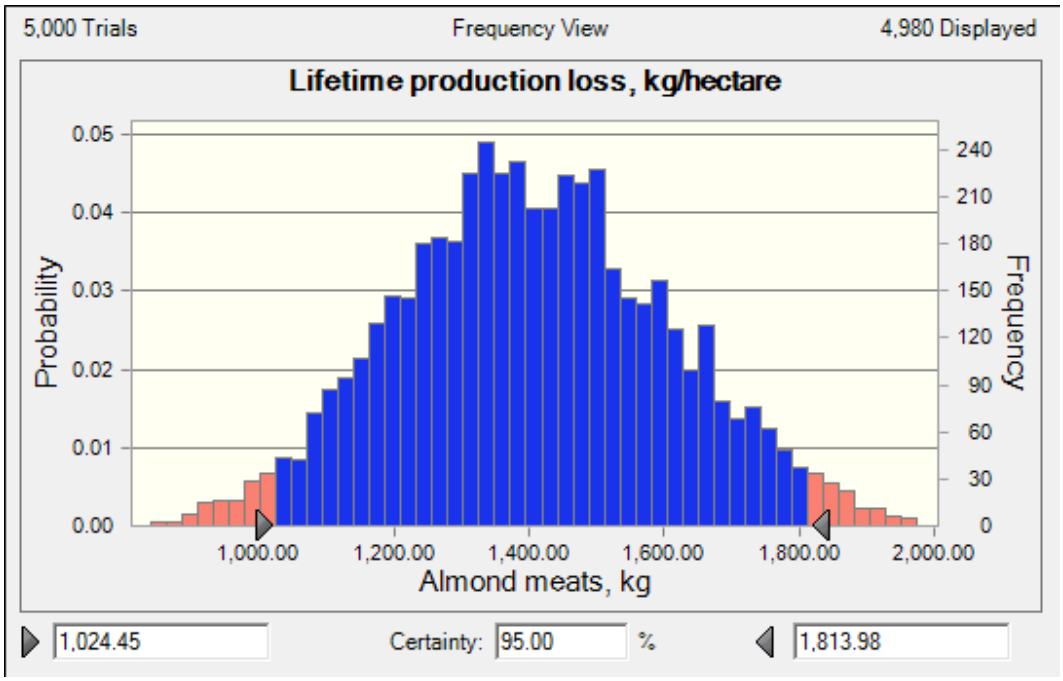

Figure 3. Simulation results for 25 years lifetime meat loss due to a 1% shaker damage/year, 95% confidence interval.

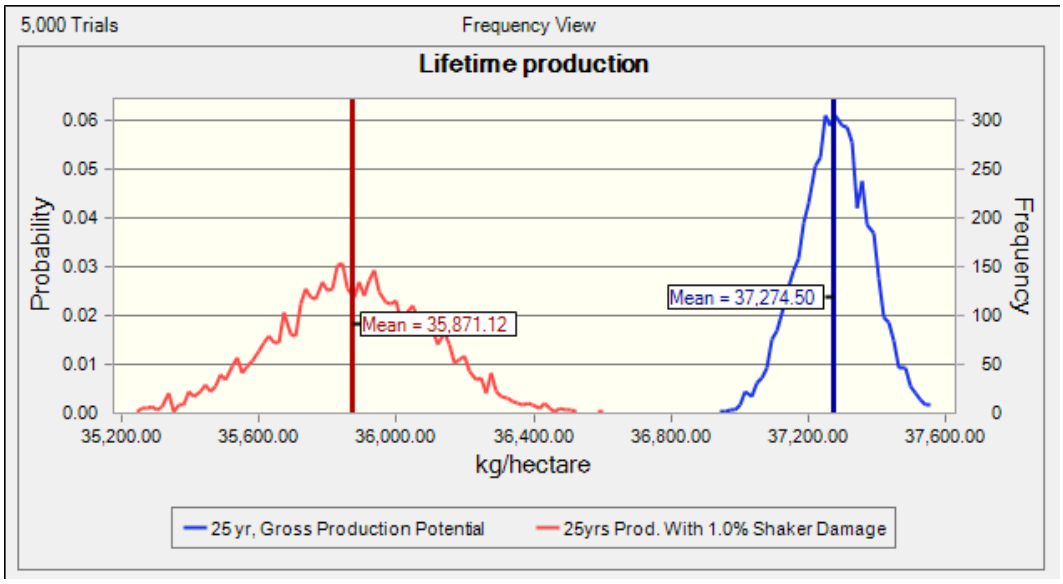

Figure 4. Simulation results for 25 years lifetime production loss and gross production potential, kg/hectare.

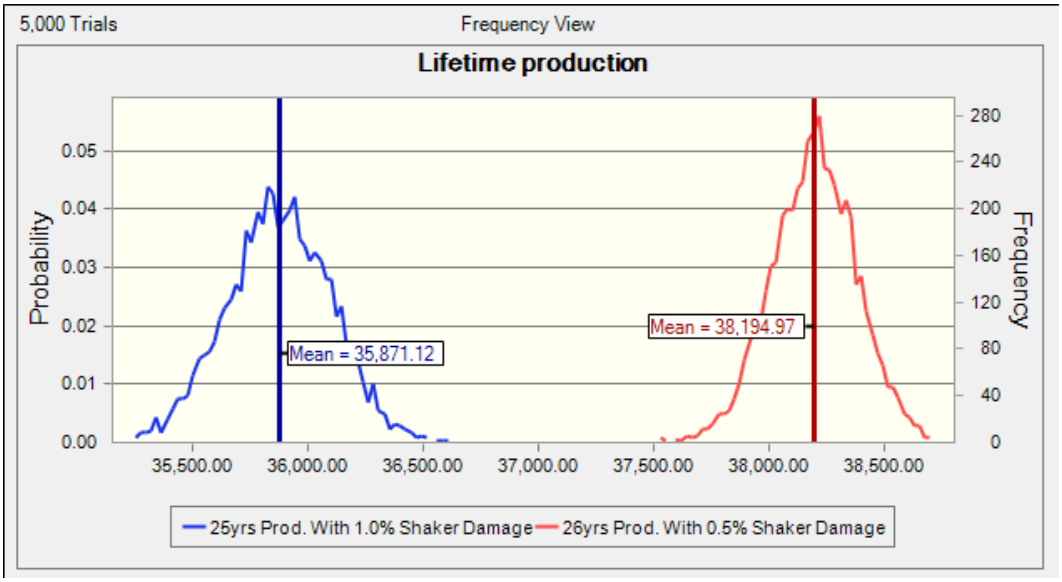

Figure 5. Lifetime production gains, meat pounds, due to 0.5% reduction in shaker damage and increased orchard life span by one year (26 years).

It could be argued that the contemporary tree shaker design is a brute force mechanical system that is significantly more powerful than needed to dislodge the crop from the tree, and the cost of this power, could be 4% total production loss over the lifetime of an orchard. Although orchard productivity is adversely affected by damage caused by mechanical tree harvesting, the tree shaker remains the most productive harvesting method for many nut and fruit crops because the benefits greatly outweigh the costs.

CHAPTER 2. TYPICAL TREE SHAKER MECHANISM

TYPICAL MECHANICAL COMPONENTS

The Magnum Shaker head, manufactured by the Orchard Machinery Corporation (Orchard Machinery Corporation, 2007), is typical example of the nut and fruit harvesting industry (Figure 1

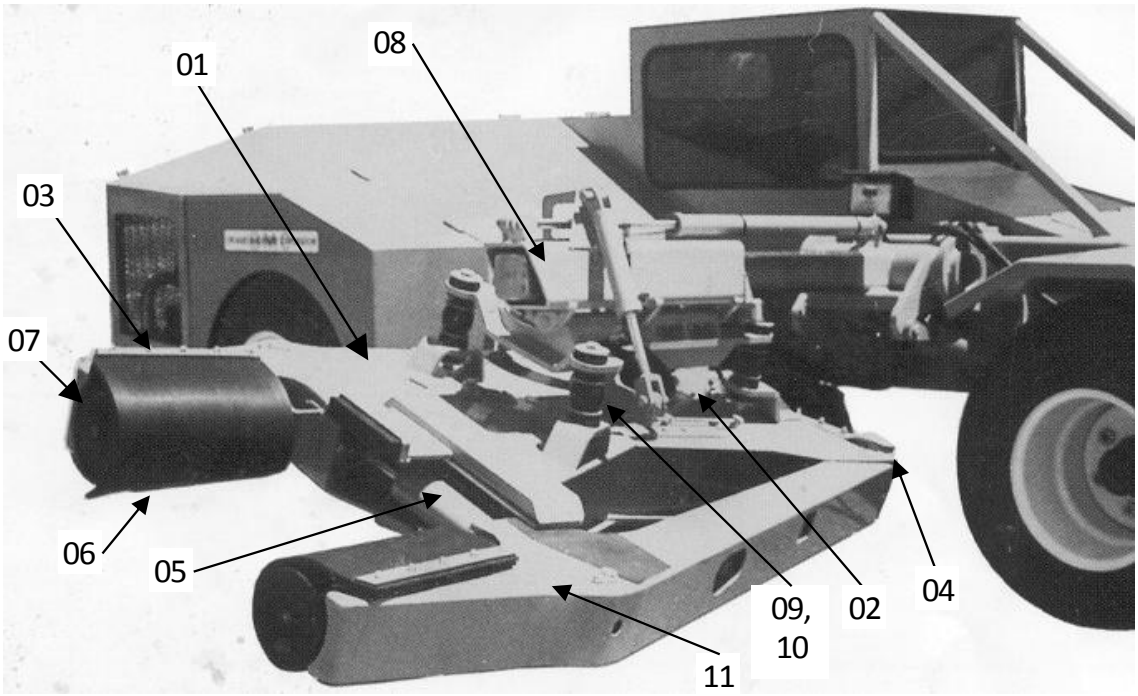

Figure 6. Orchard Machinery Corporation (OMC) side mount tree shaker with Magnum head.

and Figure 6). The current tree shaker platforms consist of a hollow welded steel case structure (Figure 6 - 01) containing the drive sheave, drive belt, two or more eccentric rotating masses commonly referred to as energy-wheels, hydraulic clamp cylinder(s), and hose routings. The hydraulic drive (Figure 6 - 02) motor mounts to the top of the case structure and is connected to the drive pulley. The tree trunk clamping super structure is an integral part of the case structure housing (Figure 6 - 03). A pivot pin (Figure 6 - 04) at the rear of the case structure attaches the clamping arm

(Figure 6 - 11). Opposing the case structure is the clamp arm. The clamping arm applies a compressive force during the shaking process when hydraulic oil causes the hydraulic cylinder to retract (Figure 6 - 05) and pivots the clamp arm about the pivot pin. A sling set (Figure 6 - 06) and pads (Figure 6 - 07) are mounted on the clamp arm and the case structure. The shaker head is suspended from a hanger frame (Figure 6 - 08) by a series of rubber isolators (Figure 6 - 09), C-bars (Figure 6 - 10), or chains (not shown), allowing the shaker head to be lifted, tilted, and rolled similar to the motions of the human shoulder, wrist, and forearm, respectively. Proper clamp angle is important to prevent adverse preload on the tree or the shaker structure. Improper clamp angle will often cause barking, and will be discussed more thoroughly in Chapter 2. Both the clamping arm and case structure contain a set of slings and pads.

The shaker-head's current assembly weight of approximately 900-kg has continually increased since its initial development in the mid-1960s. As the shaking head mass increased, the required energy-wheel mass needed to create an equivalent shaking force also increased. As will be further explained in the mathematical modeling section, this increased the moments that are developed, and therefore increased the fatigue induced by torque on the shaker housing, clamp arm and other related components.

ENERGY-WHEELS

The general agribusiness professional typically has two common beliefs about the stacked rotating eccentric mass energy-wheel system. The first belief is that when the mass force vectors align, there is an impulse. Second, when the mass force vectors are opposed, nothing happens. In other words, the belief is that the stacked rotating eccentric mass energy-wheel system is planer and all force couples cancel.

The shaker head creates the shaking force with two stacked counter rotating eccentric mass energy-wheels (Figure 7 - 12, 13). These two components are typically flame cut plates with a cylinder of steel welded to one side. The assembly is then turned, creating the bearing bores, belt grooves, and faced to provide a flat surface for mount addition weight. Two bearing mounts in

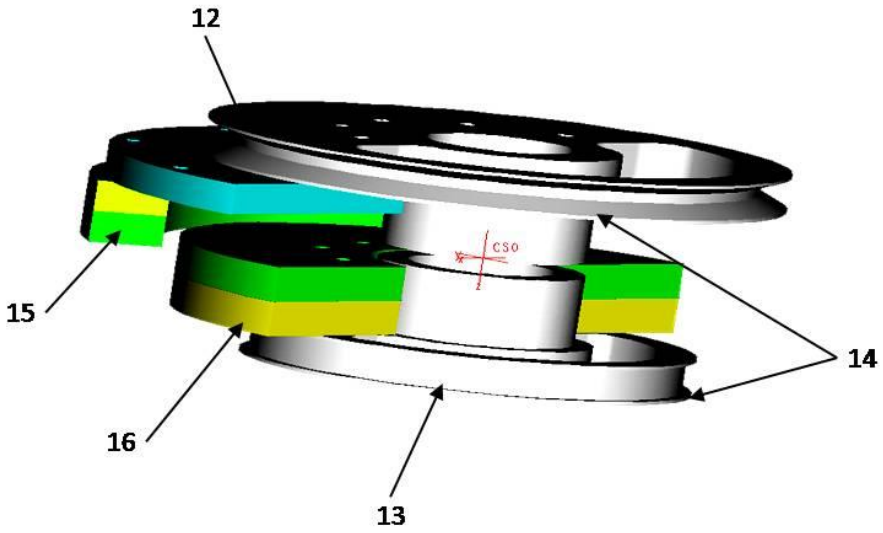

Figure 7. Typical stacked eccentric mass counter rotating energy-wheels system. The v-belt wedge drives the upper sheave, loops around an idler sheave and drives the lower sheave with the belt back, thus producing counter rotation. Weights are bolted to eccentrics to increase force.

each energy-wheel and a connecting shaft is pulled into the bearing sets of each energy-wheel after the assembly is position inside the case. The energy-wheels are stacked about the midpoint of the shaft and in the final assembly carefully locked to the upper and lower plate, and compressed between the upper and lower plate of the shaker head case. The flame cut eccentric mass plates are positioned between the head to allow the bolting on of additional weights. The additional weights bolted on (Figure 7 - 15, 16), increase the system's maximum peak force and vary the shaking pattern. The energy-wheels may have an integral drive belt (Figure 7 - 14), grooves, or a sheave (not shown) mounted to the energy-wheel. Changing the drive and driven sheaves ratios, changes the shake pattern and peak forces. The energy-wheels are typically not physically timed to the case. In the event of belt slippage, the peak forces will shift relative to prior angular orientation (ϕ). The resultant forces

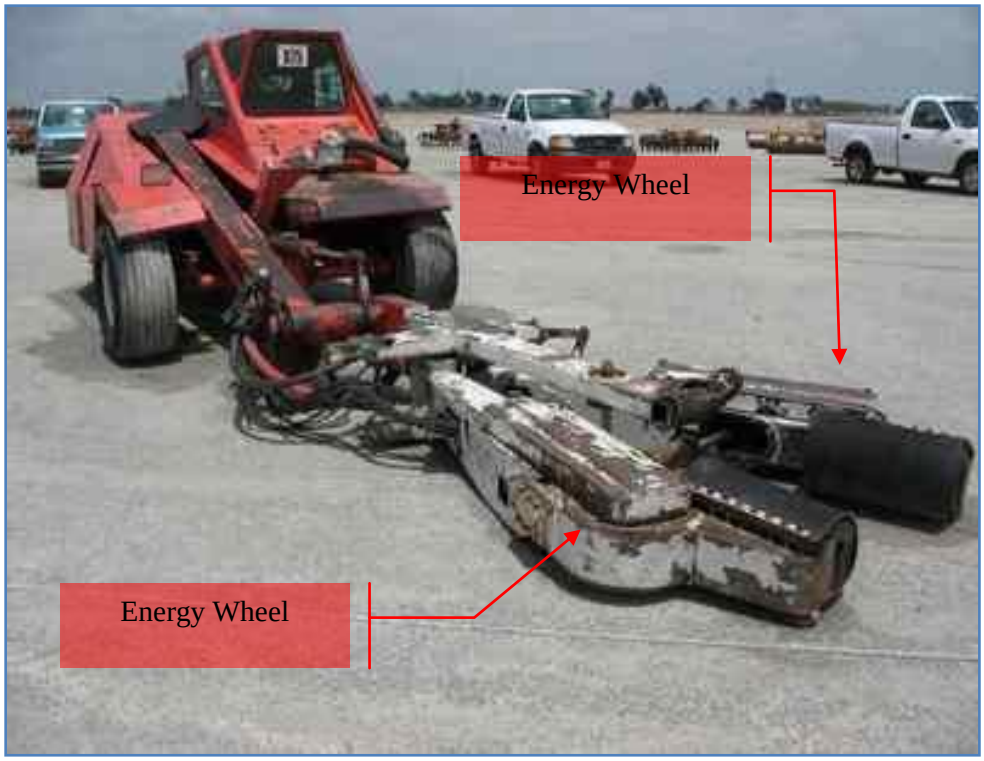

Figure 8. Used FMC three wheel, mono-boom tree shaker.

generated by the energy-wheels are transferred to the shaft at the bearings contacts and then to the housing.

Typically, the energy-wheels rotate in opposing directions, creating amplification spikes in a pattern determined by the mass and angular velocity. Although counter-rotating energy-wheels are most common, successful shaking results are also obtainable by energy-wheels rotating in the same direction at different angular velocities. Michelson (1998) for instance, suggests a method of creating a shaker pattern using two eccentric masses rotating in the same direction. Other variations include tree shaker heads previously manufactured by Farm Machinery Corporation (FMC), which have uniquely mounted energy-wheels that are unidirectional and mounted on individual shafts, in similar but opposing clamp arms that pivot about a pin located at the rear of the shaker head. A hydraulic cylinder provides closing and the

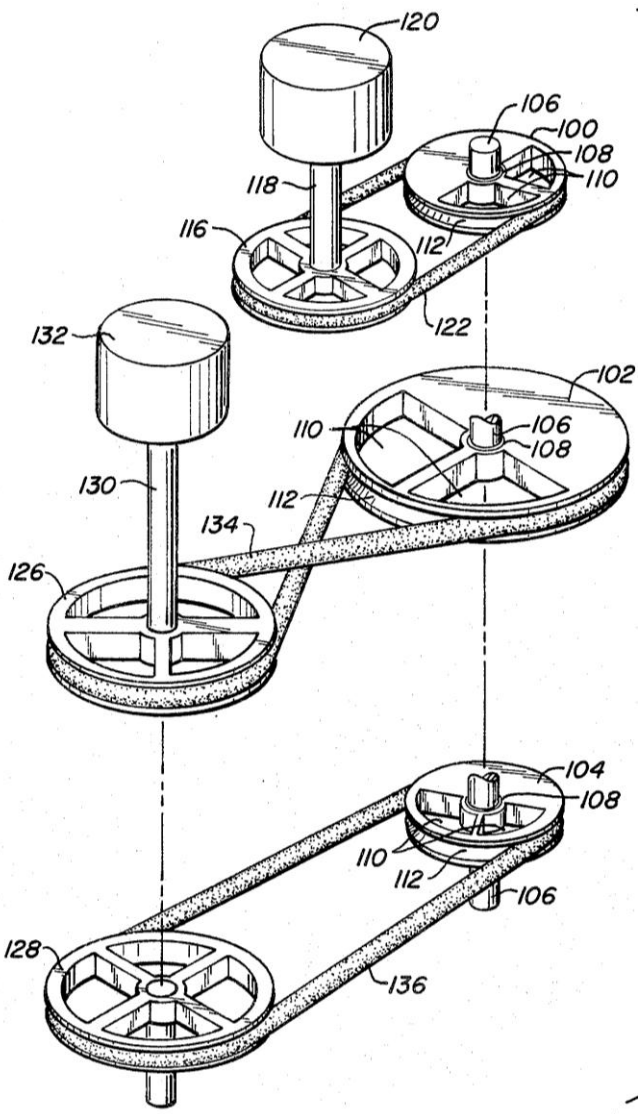

Figure 9. Westec patented, two hydraulic motors, three eccentric mass energy-wheels. Two wheels are counter rotating and the third is independent (Westerguard, 1983).

necessary clamping force during the shaking process (Figure 8). Another tree shaker manufacturer, Westec Hydraulics, introduced a third energy-wheel independently located and driven as shown on Figure 9 (Westerguard, 1983). Although touted as revolutionary, the introduction of a third energy-wheel merely added additional components to the summation equation of the forces, shown in Figure 9, and relocated the moment summation origin. Furthermore, as a rotating member, the force spikes and moments still existed, and the ability to overpower the natural tree dynamics only increased.

The development of energy wheel systems and pad and sling cooling systems account for the largest body of patents pertaining to mechanical tree shakers (Hood et al., 1979; Savage, 1981; Zehavi and Chiel, 1995; Reynolds et al., 1997; Michelson, 1998). Recent developments continue toward trying to time the energy-wheels on a single plane to eliminate all negative forces, (Zehavi and Chiel, 1995; Zehavi and Chiel, 2005). The systems developed currently use timing and structural constraints to contain the undesirable force associated rotating energy-wheel systems.

PADS, SLINGS, AND LUBRICATION

The typical tree shaker head is hydraulically clamped to the tree, engaging the outer sling to the tree bark. The inner sling, commonly cut from rubber belting, is looped around the shaker pad, locating the pad with respect to the shaker head and clamp arm structure (Figure 10). The outer and inner slings provide a semi-non-rigid connection between the tree and the mechanical tree shaker. The operator regularly lubricates the contact surfaces between the outer and inner slings with high temperature grease, silicone, or other lubricants to reduce the coefficient of friction and prevent excessive heat generation. During the clamping, depending on the operator and tree structure, the slings will allow the shaker head and the tree to move into alignment. This aligning may cause the shaker head to pitch, roll, or slide up or down on the tree trunk. Deflection of the tree also regularly occurs during the clamping process. If the movement of the tree shaker head is large, the shaker head,

or possibly the entire tree shaker, should be repositioned to prevent adverse preloading of the tree trunk.

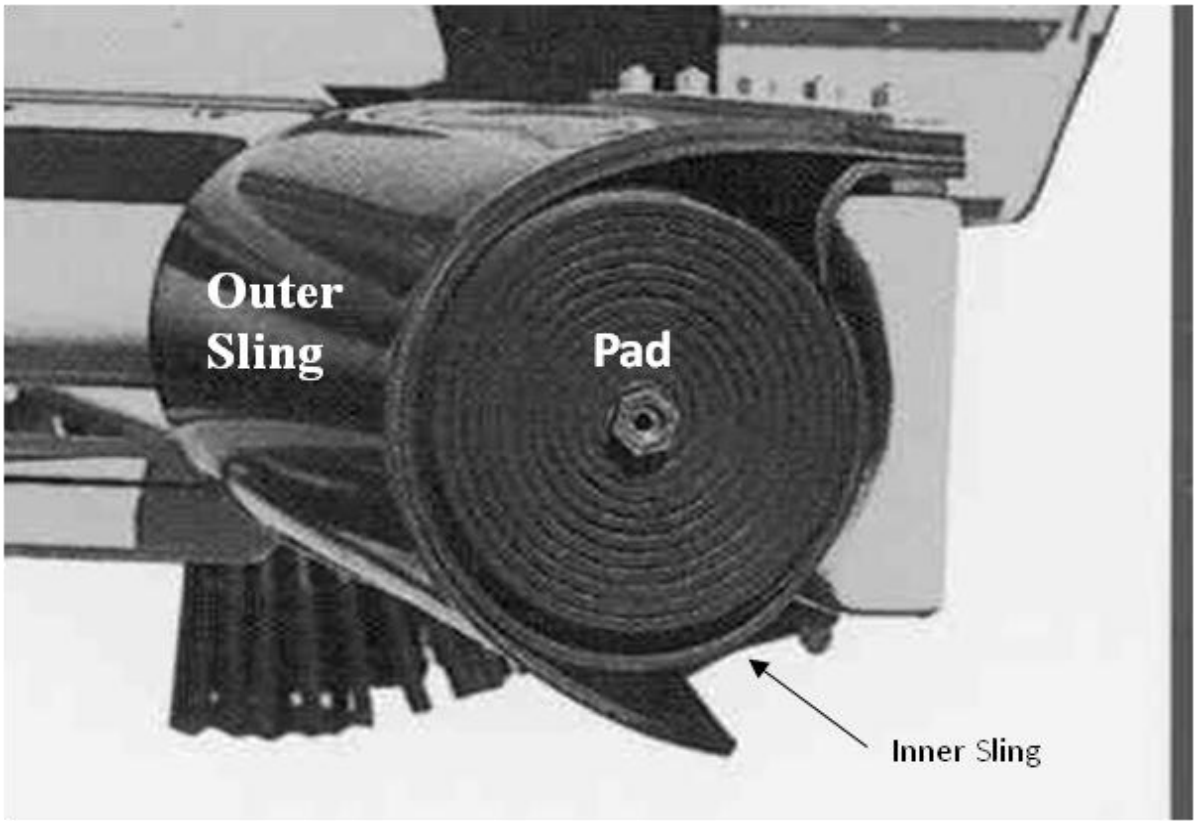

Figure 10. Tree shaker pad system with shell-filled air-cooled pad, inner positioning sling, and outer slip sling.

Depending on the style of shaker pad and clamping pressure, various amounts of pad deformation will occur when securing the shaker mechanism firmly to the tree. This deformation around the trunk is important to maximize the transfer of forces to the tree. Reducing sling friction also prevents barking by limiting the transmission of unwanted shaker head forces that are non-normal to the clamped surface of the pad. Non-normal forces are the forces that induce slipping between the inner and outer slings. Thermal buildup in the sling and pads represents inefficiencies in the system that must be dissipated. The reduction and control of friction and thermal generation has

been the focus of many patents and lubrication strategies, (Compton, 1990a; Compton, 1990b; Reynolds et al., 1997; Chiel and Zehavi, 1998). One current production strategy blows compressed air through the pads to dissipate heat from the system and further form the shaker pads to the trunk diameter (McCrill, 1992).

The sling and pad system has been sufficiently refined to generally prevent damage to many varieties of tree. Yet there are instances where tree damage with the current pad and sling system is too severe for mechanical tree shaking. Pinecone seed harvest is one example of a crop to which the sling and pad system fail to prevent critical trunk damage during harvest. Instead, a hole must be drilled through the trunk, long bolts inserted, and acorn nuts attached and tightened on both ends. A custom shaker pad that accepts the acorn nuts allows the shaker head to clamp to the tree, preventing damage during the shaker engagement. This extreme method allows for the mechanical harvesting of the pinecone seed crop, (McConnell and Edwards, 1990; Srivastava et al., 1996). For some trees, the mechanical tree harvester remains too damaging for economic gain. Other inventors propose permanently attaching a threaded rest pad to the trunk of trees so that the forces of the tree shaker are transmitted to the hardwood, thus preventing damage to the bark (Ferrari and Evans, 2002).

Working from a theoretical perspective, one must ask, "If lubrication of the slings is very important to the prevention of trunk damage, what are the unwanted forces this lubrication is intended to eliminate?" Assuming the surface interaction between the inner and outer sling is frictionless, then only the force's normal to the (y-z) plane are utilized (Figure 11). Continuing this assumption, one then confronts the performance value of the remaining forces, F_y, F_z, and moments about M_x, M_y, and M_z (Figure 12). Since the intent of the lubrication is to allow the inner and outer sling to slide versus transferring force, if these forces are detrimental, then eliminating these apparently undesired forces would 1) reduce input energy required, 2) eliminate or significantly reduce biological component damage, and 3) reduce or eliminate economic losses due to excessive abuse to permanent tree assets.

Understanding the energy-wheel system with the existence of both axial forces and moments will be beneficial in understanding the function of the current pads, slings, and lubrication systems.

Furthermore understanding the true dynamic system of the energy-wheel system will support further developments that will expand the production capabilities of mechanical tree harvesting.

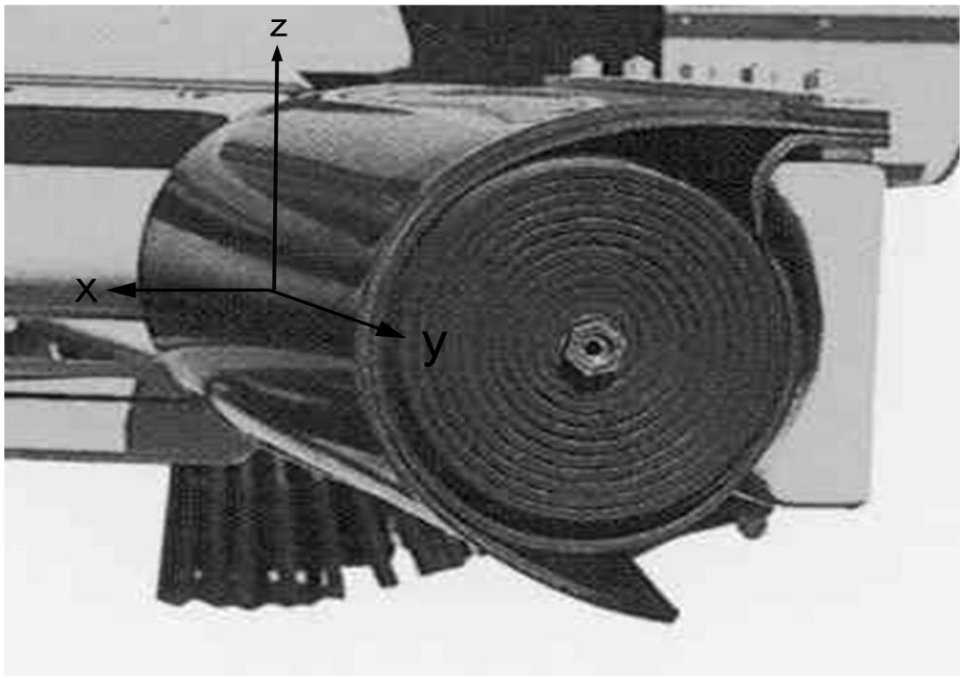

Figure 11. Reference coordinate system relative to the slings and pads.

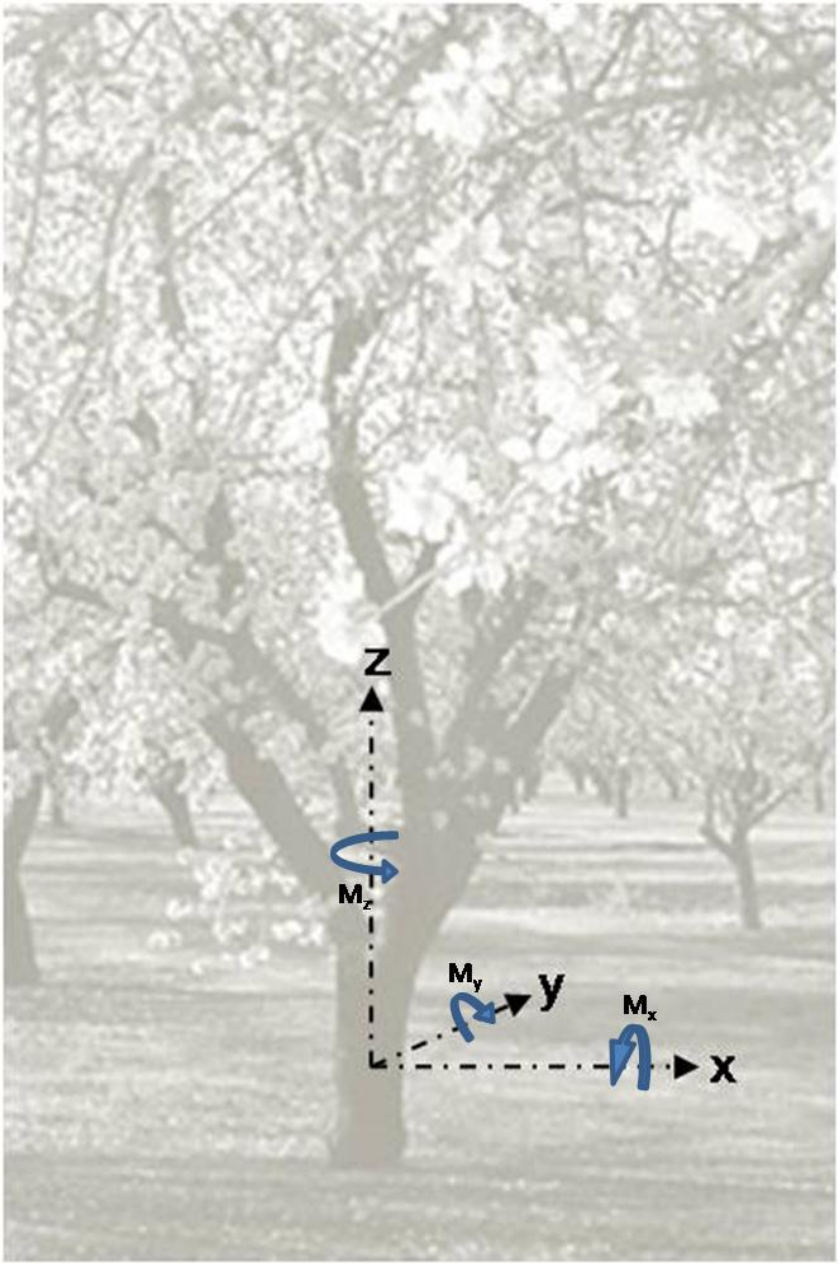

Figure 12. Reference coordinate system relative to tree.

OBJECTIVES

The fundamental rationale behind this work is that failure to recognize the moment forces has prevented the industry from attaining the required understanding to design improved next-generation tree shakers. The goal of this study was to understanding the dynamics of the energy-wheel system, and ultimately utilizing that knowledge for the development of more efficient and effective shaking systems that will increase the productive life of an orchard.

The specific objectives of this study were:

1. To explore the limitations of the planer model.
2. Expand the planer model to include moment magnitudes.
3. Analyze the effect force transmission losses on measured tree displacement.

This expansion of the planar model to include moments allowed a true representation of shaker pattern in terms both planer forces and resultant moments due to coupled forces.

CHAPTER 3. ENERGY-WHEEL FORCES

VARIABLE DEFINITIONS[ii]

a - Acceleration, m/s^2 , (ft/s^2)

a_r - Radial acceleration, m/s^2 , (ft/s^2)

cg_{zl} - Lower energy-wheel cg z-axis location, m (ft)

cg_{zu} - Upper energy-wheel cg z-axis location, m (ft)

d - Drive pulley diameter, m (ft)

D_l - Lower energy-wheel drive sheave diameter, m (ft)

D_u - Upper energy-wheel drive sheave diameter, m (ft)

F - Force, N (lbf)

$\mathbf{F_l}$ - Force matrix for lower energy-wheel, N (lbf)

$\mathbf{F_u}$ - Force matrix for upper energy-wheel, N (lbf)

$\mathbf{F_s}$ - Sum of forces, N (lbf)

g - Gravity

M - Moment, N*m (lbf*ft)

m - Mass, kg (slug)

m_l - Mass, lower energy-wheel, kg (slug)

m_u - Mass, upper energy-wheel, kg (slug)

N - Motor shaft input speed, rpm

r - Radial distance relative to axis of rotation, m (ft)

r_u - Upper energy-wheel radial location of center of gravity, m (ft)

r_l - Lower energy-wheel radial location of center of gravity, m (ft)

$\mathbf{rv_l}$ - Vector to lower energy-wheel center of mass, m (ft)

$\mathbf{rv_u}$ - Vector to upper energy-wheel center of mass, m (ft)

t_e - Duration of shaking sequence, sec

t_0 - Initial time, sec

t_s - Time step for iteration, sec

z_l - Distance from midpoint of shaft to lower energy-wheel cg location, m (ft)

z_u - Distance from midpoint of shaft to upper energy-wheel cg location, m (ft)

ϕ - Phase angle, rad

ω - Angular velocity, rad/sec

θ - Change of rotation of input pulley, rad

η_x - Force transfer efficiency, x-axis, %

η_y - Force transfer efficiency, y-axis, %

η_z - Force transfer efficiency, z-axis, %

θ_l - Lower Energy-wheel position, rad

θ_u - Upper Energy-wheel position, rad

PLANER FORCES

The two-dimensional (planer) force models are regularly presented as the dynamics of the shaker head system (Srivastava et al., 1996). In this chapter, the planer models will be presented, expanded, and then further developed to disclose the moments along with the commonly explained planar forces model. The tree-shaker-head reference frame is the following:

1. X-axis is normal to the pads, slings, clamp arm, and tree centerline.
2. Y-axis is parallel to the pads, slings, intersecting tree centerline, with clamp arm orientated away from the tree shaker.

3. Z-axis is concentric to the trunk pointing skyward (Figure 11, relative to shaker head and Figure 12, relative to the tree).

The forces of the stacked energy-wheel system are developed according to Newton's second law.

$$F = m \cdot a \tag{1}$$

Acceleration comes from the rotation of an eccentric mass about a pin. The equation for this radial acceleration component is:

$$a_r = r \cdot \omega^2 \tag{2}$$

Substituting Equation 2 into Newton's second law, Equation 3 defines the force created by the energy-wheel and rigid body eccentric mass rotating about a fixed shaft.

$$F = m \cdot r \cdot \omega^2 \tag{3}$$

The angular position of the upper and lower energy-wheels can be different based on diametrical differences between the drive and driven sheave of each energy-wheel. The energy-wheel force vector can be related to the input sheave by:

$$\theta_u = \theta \cdot \frac{d}{D_u} \tag{4}$$

$$\theta_l = \theta \cdot \frac{d}{D_l} \tag{5}$$

In addition, the angular velocities of the energy-wheels are related by sheave diameters of the input, energy-wheel, and the input speed, N.

$$\omega_u = \frac{d \cdot N \cdot \pi}{30 \cdot D_u} \tag{6}$$

$$\omega_l = \frac{d \cdot N \cdot \pi}{30 \cdot D_l} \tag{7}$$

As the energy-wheels rotate, the magnitude of the x and y force components changes. Placing the forces in a matrix format will assist in the calculation of moments.

$$\mathbf{F_{xyz}} = \begin{bmatrix} F_x \\ F_y \\ F_z \end{bmatrix} = \begin{bmatrix} \cos(\theta) \cdot F \\ \sin(\theta) \cdot F \\ -m \cdot g \end{bmatrix} \tag{8}$$

The position of the drive pulley and the energy-wheels are dependent on time.

$$\theta(t) = \frac{N \cdot \pi \cdot t}{30} \tag{9}$$

For analyzing the tree shaker as a planar system, the following two matrices, Equations 10 and 11, develop the component forces for a shaker system's upper and lower energy-wheels as a function of the angular change of the cg location about the shaft of rotation. The negative sign in front of θ (Equation 11) represents the counter rotation of the lower energy-wheel. Finally, the introduction of efficiency variables η_x, η_y, and η_z represents force transmission efficiencies.

$$\mathbf{F_u(t)} = \begin{bmatrix} \cos\left((\theta(t)+\phi)\cdot\frac{d}{D_u}\right)\cdot m_u\cdot r_u\cdot\left(\frac{d\cdot N\cdot\pi}{30\cdot D_u}\right)^2\cdot\eta_x \\ \sin\left((\theta(t)+\phi)\cdot\frac{d}{D_u}\right)\cdot m_u\cdot r_u\cdot\left(\frac{d\cdot N\cdot\pi}{30\cdot D_u}\right)^2\cdot\eta_x \\ -m_u\cdot g\cdot\eta_z \end{bmatrix} \quad (10)$$

$$\mathbf{F_l(t)} = \begin{bmatrix} \cos\left(-(\theta(t)-\phi)\cdot\frac{d}{D_l}\right)\cdot m_l\cdot r_l\cdot\left(\frac{d\cdot N\cdot\pi}{30\cdot D_l}\right)^2\cdot\eta_x \\ \sin\left(-(\theta(t)-\phi)\cdot\frac{d}{D_l}\right)\cdot m_l\cdot r_l\cdot\left(\frac{d\cdot N\cdot\pi}{30\cdot D_l}\right)^2\cdot\eta_x \\ -m_l\cdot g\cdot\eta_z \end{bmatrix} \quad (11)$$

Equation 12 is the summation of Equations 10 and 11 results in the theoretical pattern often published as the resultant effect of two rotating eccentric masses energy-wheels, as shown in Figure 13 (Orchard Machinery Corporation, 2007). Equation 12 can also be expanded to include additional energy-wheels, $F_n(\theta)$ and can be utilized for analysis of any suggested shaker energy pattern.

$$\mathbf{F_s(\theta)} = |\mathbf{F_u(\theta)} + \mathbf{F_u(\theta)} + \cdots + \mathbf{F_n(\theta)}| \quad (12)$$

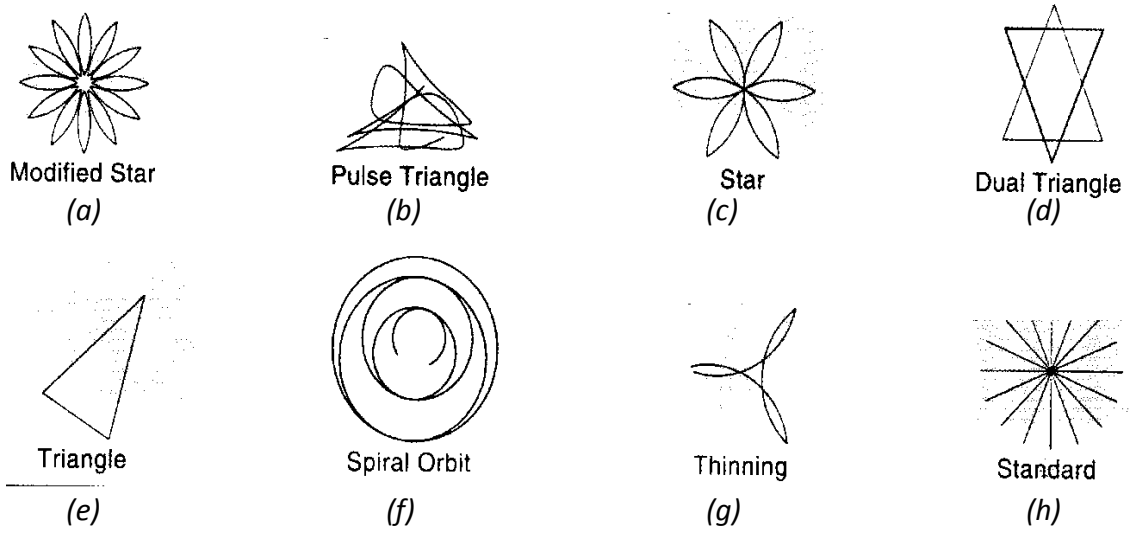

Figure 13. Orchard Machinery Corporation (OMC) advertised shaker head energy patterns.

Modifying the shaker patterns has been a successful option to create different tree shaking dynamics. Changing the pattern shape, i.e. increasing or decreasing the number and magnitude of impulses is a function of:

1. Sheave ratios, driver and driven
2. Adding or subtracting weight from the upper, lower, or both energy-wheels
3. Increasing or decreasing the input rpm
4. Increasing or decreasing the energy-wheel center of gravity (cg) radial position relevant to the axis of rotation.

However, the patterns shown in Figure 13 are not all direct outputs of Equation 12. Five of the eight patterns, the modified star (a), star (c), triangle (e), spiral orbit (f), and thinning (g), are mathematically possible planer shaker patterns using Equation 12. A set of simple system parameters including sheave diameters and/or the energy-wheel weights to achieve shaker patterns similar to those published by Orchard Machinery Corporation has been defined in Table 4.

Both the pulse triangle and the dual triangle will be discussed in detail later. The standard pattern (h) presents an interesting concept suggesting planer forces can be linearized. Furthermore, when the force vectors are opposed, the systems are instantaneously indexed to rotate the pulse about the truck's z-axis (Figure 12). Timing of the energy-wheels is a special condition that is also included in Table 4 and requires the weight, angular velocity, and energy-wheel cg location be identical. This special and simplified concept of a linearized energy-wheel system will be used later to develop the initial concept moments.

Table 4. Sheave diameters and eccentric wheel weights used to generate theoretical shaker patterns.

Pattern Name	Upper Sheave Diameter, m	Lower Sheave Diameter, m	Upper Energy-Wheel Weight, kg	Lower Energy-Wheel Weight, kg	Figure Number
Modified Star	0.51	0.61	45.4	47.7	Figure 14
Star	0.46	0.61	33	47.7	Figure 15
Thinning	0.31	0.61	12.3	47.7	Figure 16
Spiral Orbit	0.25	0.61	22.7	22.7	Figure 17
Triangle	0.31	0.61	7.7	47.7	Figure 18
Linear	0.61	0.61	47.7	47.7	Figure 22

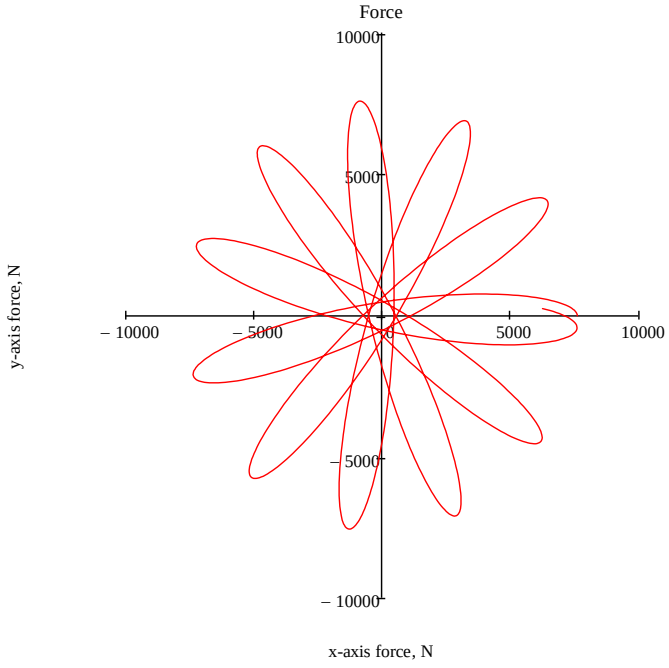

Figure 14. Modified star pattern plot using Equation 12 and values from Table 4.

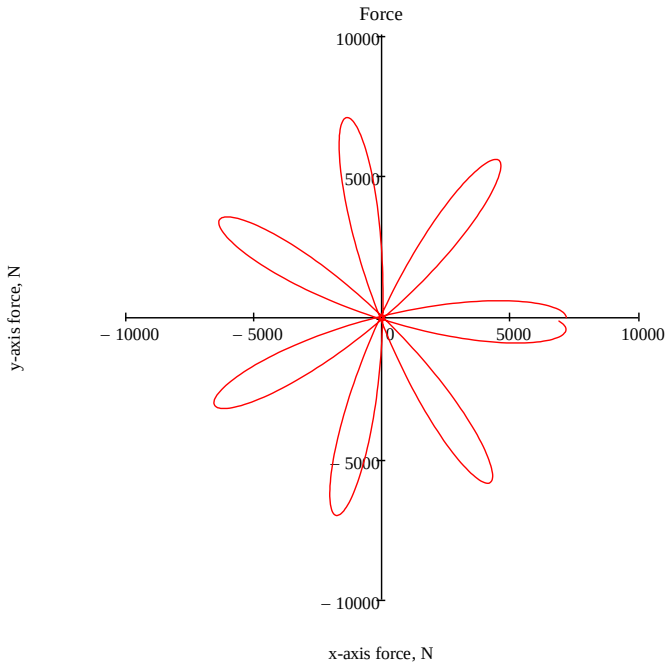

Figure 15. Star pattern plot using Equation 12 and values from Table 4

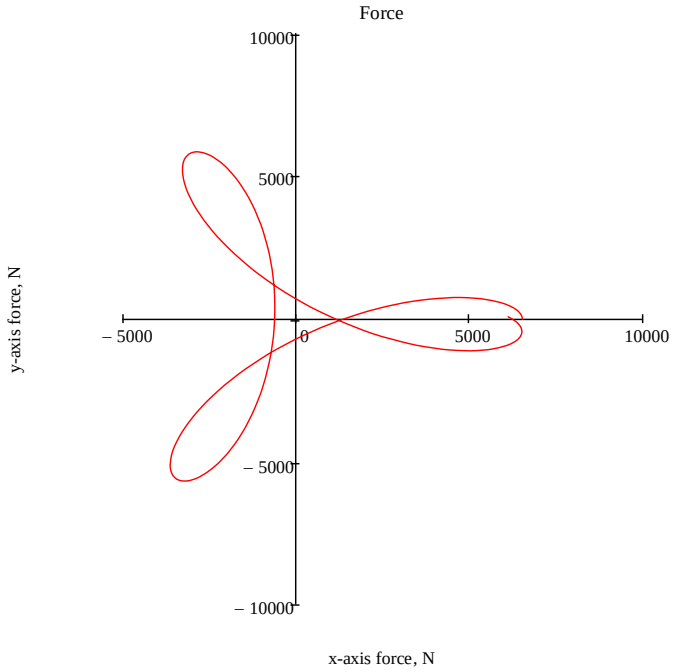

Figure 16. Thinning pattern plot using Equation 12 and values from Table 4.

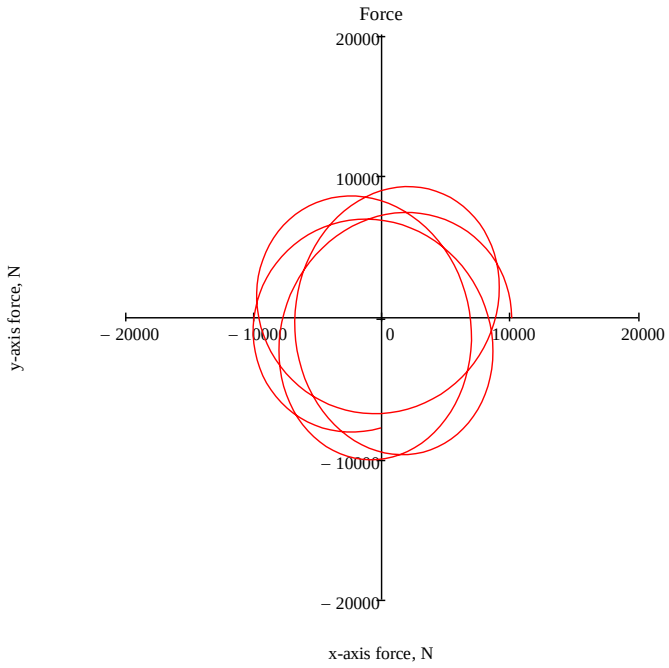

Figure 17. Spiral Orbit pattern plot using Equation 12 and values from Table 4.

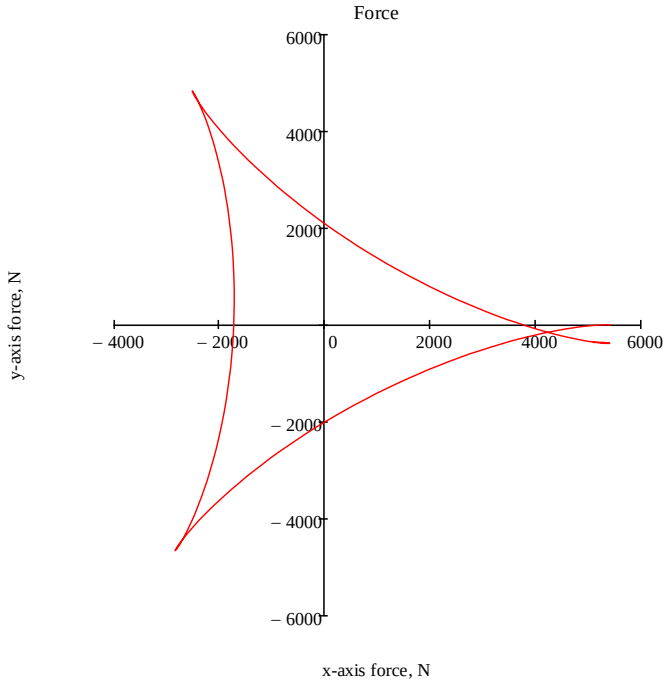

Figure 18. Triangle pattern plot using Equation 12 and values from Table 4.

The final three patterns Figure 13 (b, d, h) cannot be mathematically realized based on equation 12. However, these suggested patterns will be useful in the understanding of several facts about stacked eccentric mass energy-wheel systems, including; 1) there are extensive force transfer losses due to the suspension system, 2), the independent rotating energy-wheels or stacked energy-wheel systems do not result in independent reaction forces at the shaker head and tree interface, and 3) linearization of the system does not result in only normal forces. Therefore assuming cancellation of all other forces created by stacked counter rotating energy-wheel systems is invalid.

Realistically, the Pulse Triangle shown in Figure 13 (b) reflects a triangular planer pattern when all of the resisting and restoration forces are considered. Resistant and restoration forces are the tree transportation hangers, hydraulic hoses, and the tree (Figure 19). The complexity of the geometric representation is past the capabilities of Equation 12. Equation 12 will create a pattern that is continuous between the maximum forces, and the same shape will exist between any two force maximums. The Pulse Triangle has several force maximums and the path between each set is different. This supports that there are additional forces acting on the system.

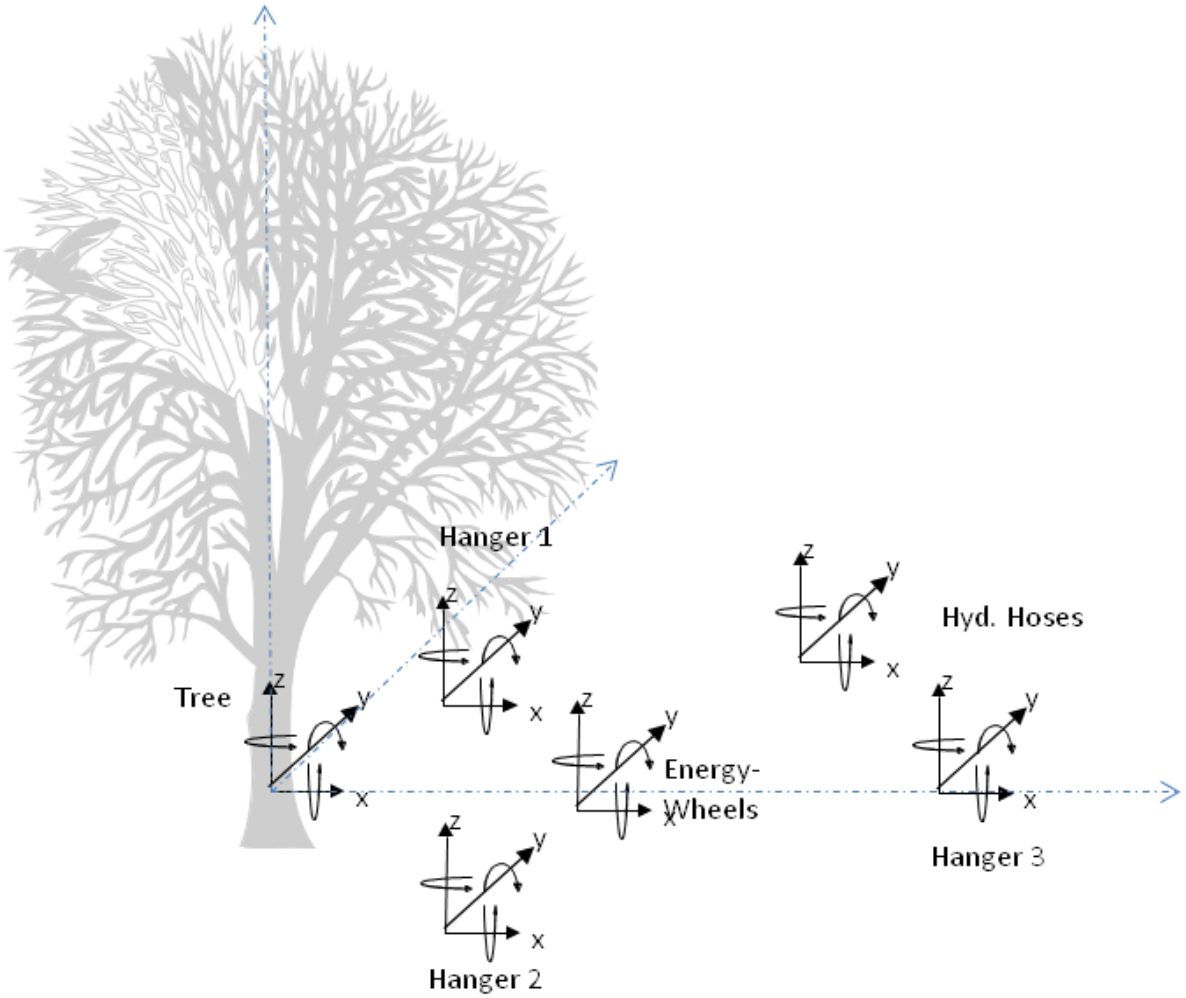

Figure 19. Reaction forces

Abdel-Fattah (2003) research provides a series of plots showing the x and y displacements of a shaker head in a free state and attached to the tree trunk (Figure 20). The lower series of results, shaker D4 – a, b, and c, is very representative of the modified star. As is clearly seen, the loops and crossing patterns are reminiscent of the modified star pattern shown in Figure 14. However, the Free Shake plot (Figure 20 (a)) does not reflect the uniformity of the mathematical plots derived from Equation 12, but indicates that the actual system displacement must have constraints, and

displacement losses. The Free Shake plots shows the mechanical loss associated with the suspension system consisting typically of three hangers and hoses connected to the hydraulic drive motor.

The center and right plots of Figure 20 demonstrate the difference between the shaker head and tree displacement during the shaking. This represents transmission losses in the pads and slings. The x-axis sees little loss of magnitude between the shaker head and the tree trunk displacement, while the y-axis sees a significant displacement reduction. Abdel-Fattah (2003) found that the relative average displacement of the y-axis to x-axis for all shakers tested was, on average, 66%. For the D4 shaker data the tree displaced 9.1mm in the x-axis and 5.9mm in the y-axis. The tree diameter is 18.1cm and the tree shaker was clamped to the tree at a height of 60cm. Remembering the slings are lubricated to allow slippage between the tree and shaker head, the expectation is transmission of forces parallel to the lubricated surface are reduced.

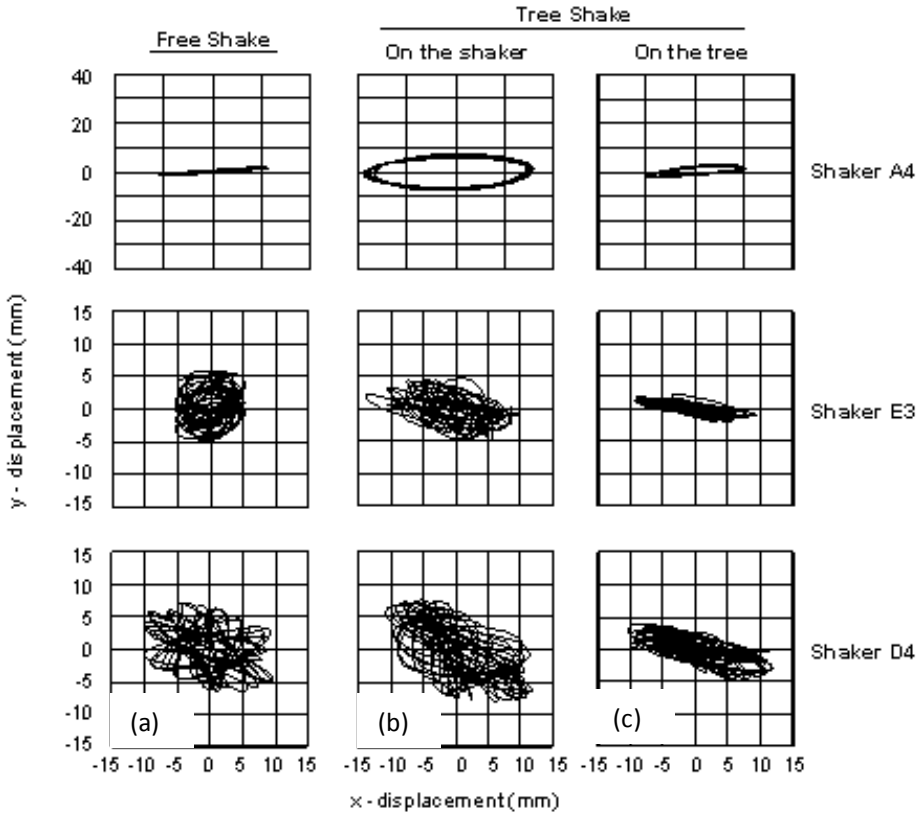

Figure 20. Plots of measured displacement for almond trees (Abedel-Fattah, 2003)

The Dual Triangle shaker head pattern shown in Figure 13 (d) indicates that two independent triangular patterns can be created and operated as independent systems. The suggestion that there are two independent triangular patterns as shown by the Dual-Triangle implies two sets of counter rotating energy-wheels timed in such a manner to produce independent resultant forces. The Dual Triangle and Standard pattern are not mathematically supported (Figure 13) and a double set stacked counter rotating energy-wheels platform has never existed.

Figure 21 shows the plot of the initial triangular shaker pattern ϕ equals 0 degree in Equation 10 and 11. The second independent triangle is plotted by setting ϕ to 120 degree. The total forces of two linked "independent" triangle energy systems each represented by Equation 12 can be represented by the expanded , Equation 13.

$$\mathbf{F_s(t)} = |[\mathbf{F_u(t)} + \mathbf{F_l(t)}] + [\mathbf{F_{2u}(t)} + \mathbf{F_{2l}(t)}]| \tag{13}$$

Plotting the first and second independent energy-wheel systems simulates the advertised shaker pattern (Figure 13). The summation of the two proposed independent energy-wheel systems, contained in a common structure and acting on a single tree, results in the summation of vector forces in a resultant vector force, at the tree trunk interface (Figure 21).

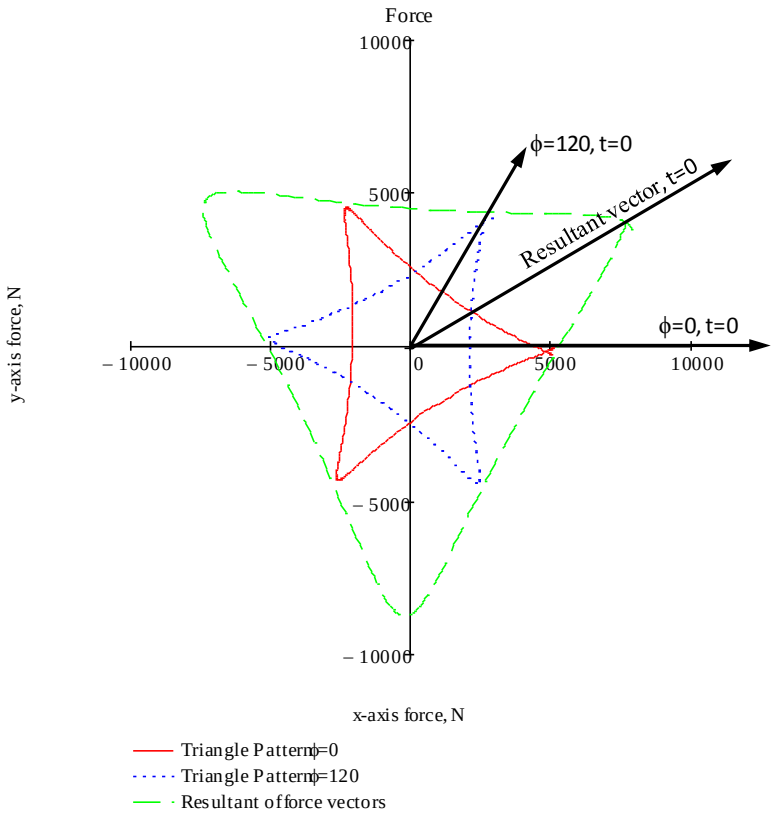

Figure 21. Dual Triangle pattern results in a single applied force to the tree when contained in a common structure.

The final misleading energy pattern is the standard (Figure 13 (h)). The standard pattern assumes a stacked energy system can have a bi-directional linear pulse. The pulse force then is somehow incremented about the z-axis applying a linearized force in a different planer direction. The common belief is that timing the eccentric mass energy-wheels system produces a bi-directional pulse. To simulate a bi-directional pulse using Equation 12 the following constraints must exist:

1. Both the upper and lower energy-wheel must have the same mass.
2. The location of the center of gravity of the upper and lower energy-wheel must be located the same radial distance from the common shaft.
3. The energy-wheel must be counter rotating.

4. The energy-wheels must have the same angular velocity.
5. Finally, the energy-wheels must be timed to the shaker head case so as to produce only force in the x-axis, normal to the sling lubricated surface.

Figure 22 shows the results of these assumptions. The forces are normal to the shaker head and the y-axis planer forces sum to zero. The desire of the industry to have a system with no non-normal forces is the belief that non-normal forces are damaging and therefore must be minimized to prevent tree damage.

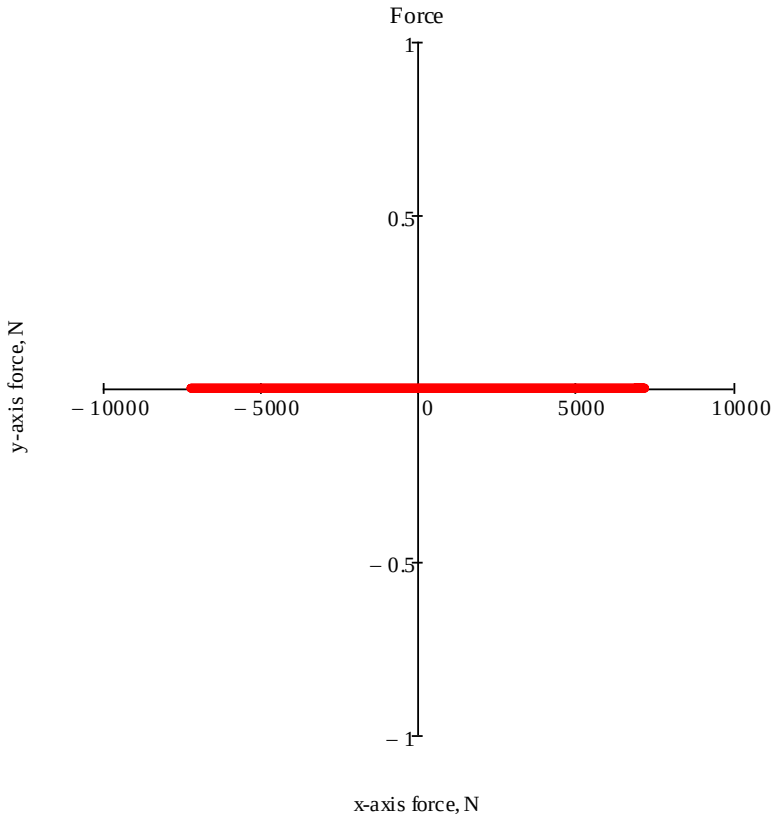

Figure 22. Linear shaker pattern

MOMENTS & FORCES

Abedel-Fattah (2003) states the following:

> Most commercial trunk shakers use counter-rotating masses to deliver a relatively high frequency (12-40Hz), small zero-to-peak displacement [5 to 20mm (0.2-0.8in)] shaking pattern to the trunk in the horizontal (x-y) plane.

Throughout the history of mechanical tree shaking force analysis has been simplified to a planer system, the existence of a moment remains undisclosed. Visual existence of moments is easily observed by watching a shaker head video in slow motion. The shaker head can be observed making abrupt torsional movements, in addition to the standard planer displacement forces commonly discussed. However, current engineering handbooks (Stout, 1999), published papers, and patents fail to introduce the moments that exist during the rotation of two stacked eccentric masses energy-wheel system. Believing the system is planar, inventors such as Zehavi and Chiel (1995) pursue both simple and complex methods of the timing of energy-wheels, believing that timing will eliminate all unwanted forces. This is a very common, if not universal belief, that the typical stacked counter rotating eccentric mass energy-wheel system output forces that simply result in the amplification and cancellation of planer forces.

The stacked counter rotating eccentric mass energy-wheel system transfers rotational energy into planer forces and moments. A moment exists when a force act upon a lever and even though it appears the stacked shaker head system has no lever, it does, two in fact. The lever in the stacked energy-wheel system is the vertical distance from the system origin to midpoint between each energy wheel bearing set, denoted as z_u and z_l in Figure 23. Although the lever is relatively short, the force applied is large and results in a significant moment. This moment is large enough to cause the shaker head to be seen visually rotating during the shaking process.

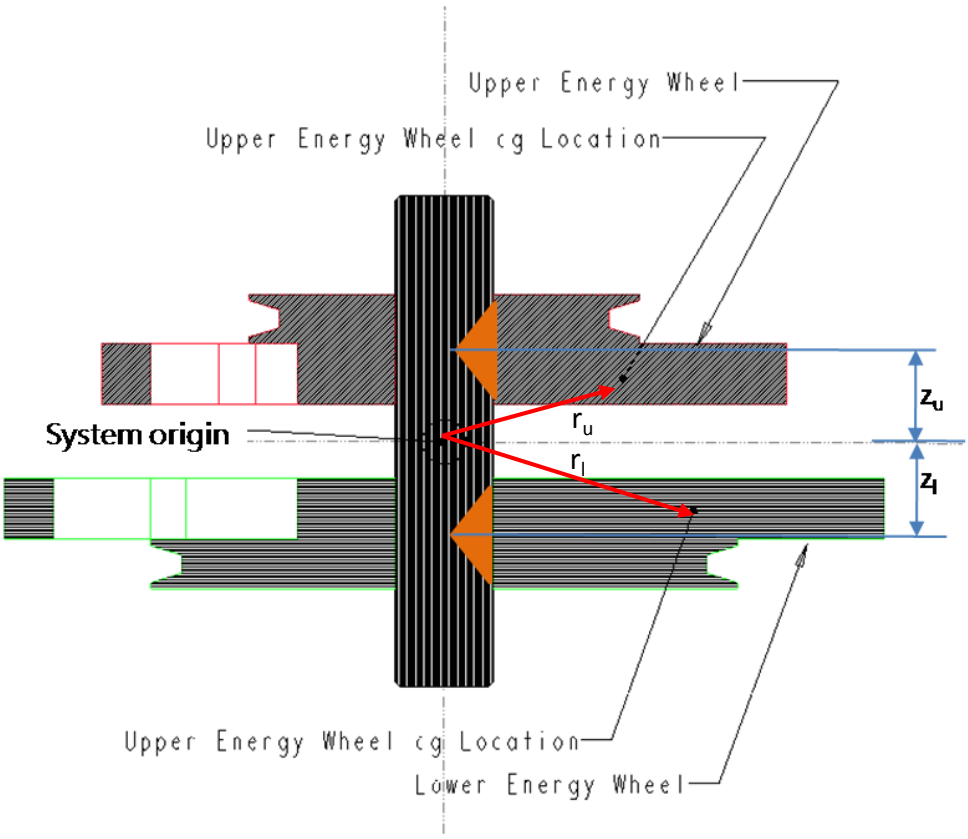

Figure 23 Section of a typical energy-wheel assembly.

Using the established variables for the Modified Star pattern Table 4, the upper and lower energy-wheels have a calculated radial force of 4092 and 5581 N respectively. With a lever arm of 4 cm the resultant moment would be 387 N m. Using a similar analysis as the planer forces, one can easily understand that the moment maximum is when the eccentric masses are opposing and the minimum is when the eccentric energy-wheels are aligned. The cross product of the lever arm and the force matrix is used to analysis the moment magnitude, Equation 14. The lever arm r_u and r_l provide the angular orientation as a function of time and vertical position of energy-wheel contact point (Equation 15 and Equation 16). The applied forces are determined from previously developed equations for the planer system, Equations 10 and 11, and are substituted into Equation 14, yielding Equation 17.

.

$$\mathbf{M} = |\mathbf{r} \times \mathbf{F}| \tag{14}$$

$$\mathbf{rv_u(t)} = \left[r_u \cdot \cos\left(\frac{d}{D_u}\right) \cdot \theta(t) \quad r_u \cdot \sin\left(\frac{d}{D_u}\right) \cdot \theta(t) \quad z_u \right] \tag{15}$$

$$\mathbf{rv_l(t)} = \left[r_l \cdot \cos\left(\frac{d}{D_l}\right) \cdot \theta(t) \quad r_l \cdot \sin\left(\frac{d}{D_l}\right) \cdot \theta(t) \quad z_l \right] \tag{16}$$

$$\mathbf{M(t)} = |\, \mathbf{rv_u(t)} \times \mathbf{F_u(t)} + \mathbf{rv_l(t)} \times \mathbf{F_l(t)}| \tag{17}$$

A simple initial model representing the planer bidirectional system previously discussed, where the energy-wheels had the same mass, angular velocity, vertical lever arm distance, and cg location, allows for a better understanding of the relationship between forces and moments. In this idealized case, the weight of the energy-wheels is negated which will allow the moments and forces to cycle from zero to a maximum. Review of the planer plots shown in Figure 22, simply indicate that the resultant forces are bidirectional and linear. The two dimensional plot of Figure 24 provides a simple presentation of the true relationship between the planer force and the moment. As the planer force reaches a maximum, when the force vectors of the eccentric mass energy-wheels cross, the moment is zero. The maximum of the moment is when the vector sum of the planer forces is zero. The three-dimensional plot of the force and moment relationship clearly shows the system is not planer (Figure 25). In Figure 25, the original planer plot is shadowed in the x-y plane.

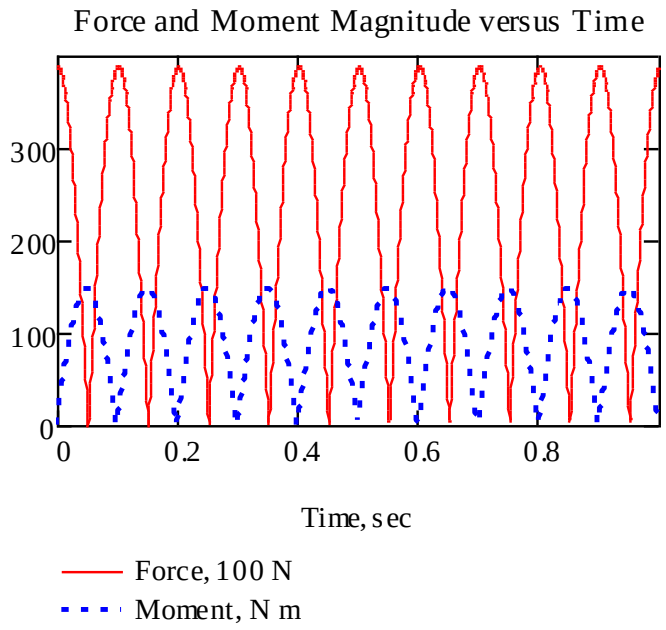

Figure 24 Two-dimensional plot, force and moment maxima and minima

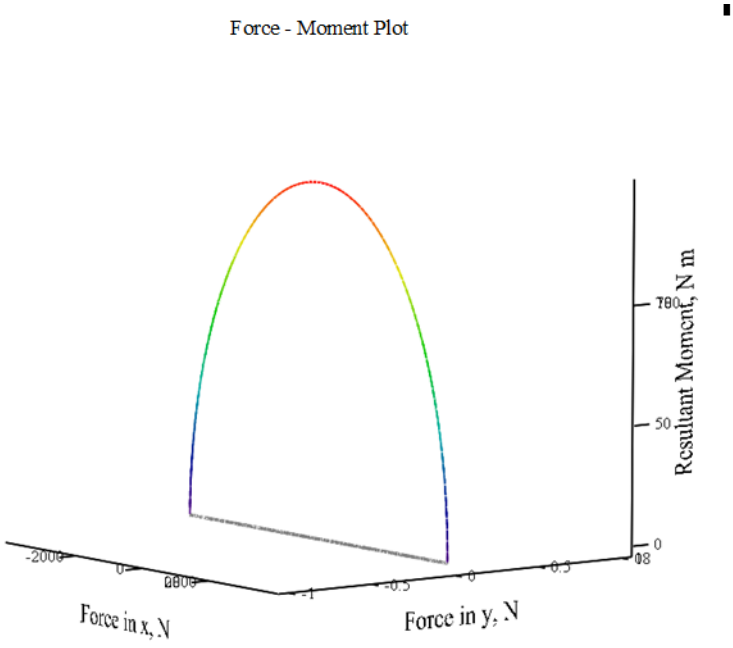

Figure 25. Bidirectional planer system, force and moment plot

In discussing the energy-wheel dynamic, it is also important to understand the moment from a reference datum and the axis "m" versus a global reference frame. In the global reference frame, the shaker head will appear to tilt, roll, and pivot about the tree. This is the result of the magnitude and direction of the moment relevant to a local reference frame. Establishing a local reference frame at the center of rotation of the energy-wheels allows plotting the moment magnitude and direction about the m-axis. What happens is when the force vectors align the direction of the moment instantaneously change direction about the m-axis. Using the simplified bi-directional linear model this change in moment direction can be easily understood.

1. At time t_0, the force vectors of both energy-wheels are aligned, and the moment magnitude is at a minimum; in this special case, the moment is zero and the entire energy transformation is planer forces Figure 26. In production energy-wheel systems a moment exists about n-axis due to different masses, angular velocity, and center of gravity location each energy-wheel.

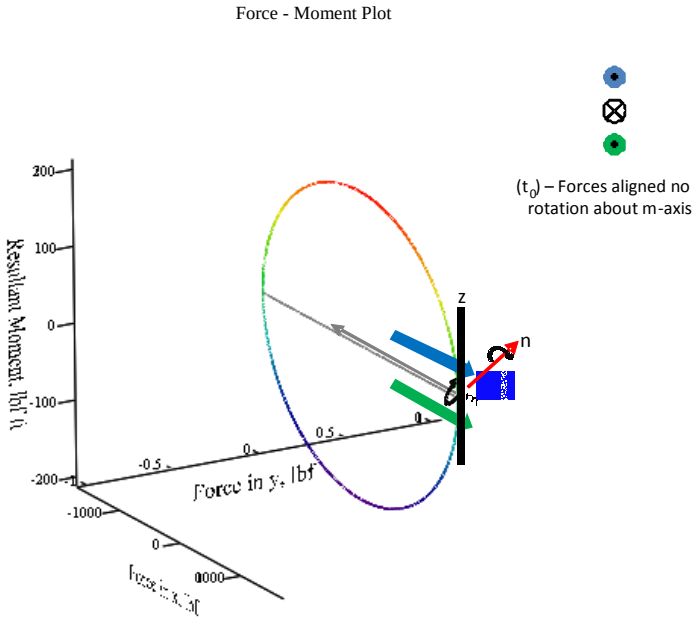

Figure 26. Force and Moment, at time t_0

2. Time, t_1, the energy-wheel force vectors are opposing and the moment magnitude is at a maximum (Figure 27). In this idealized model, all of the energy would be a moment and there would be no planer forces.

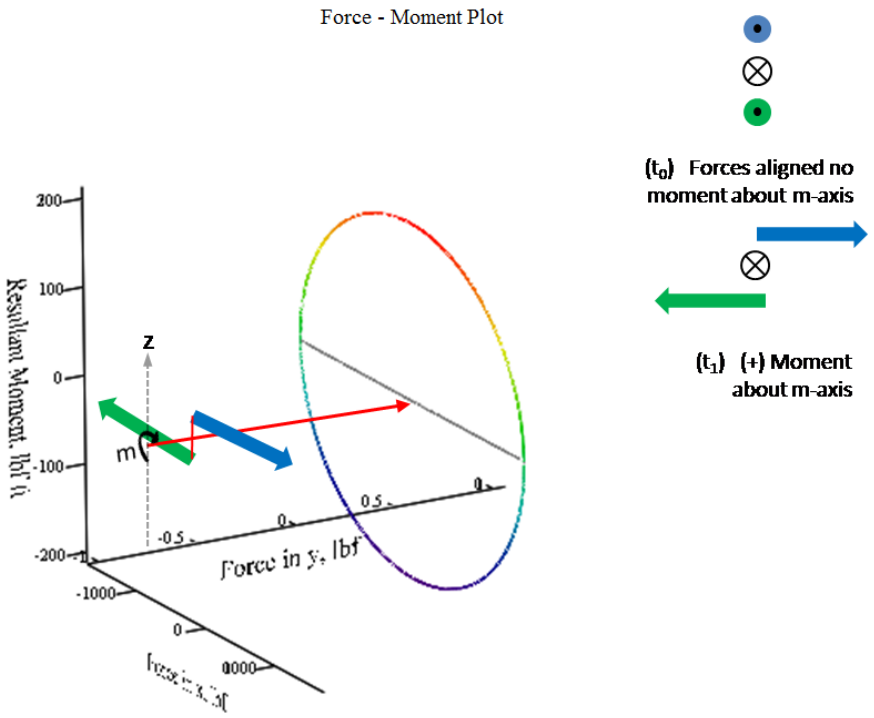

Figure 27. Force and Moment, at time t_1

3. Time, t_2, again the energy-wheel force vectors are aligned and the moment magnitude is a maximum, Figure 28. Again in a production energy-wheel system, there would be a moment about n-axis due to different masses, angular velocity, and center of gravity location each energy-wheel

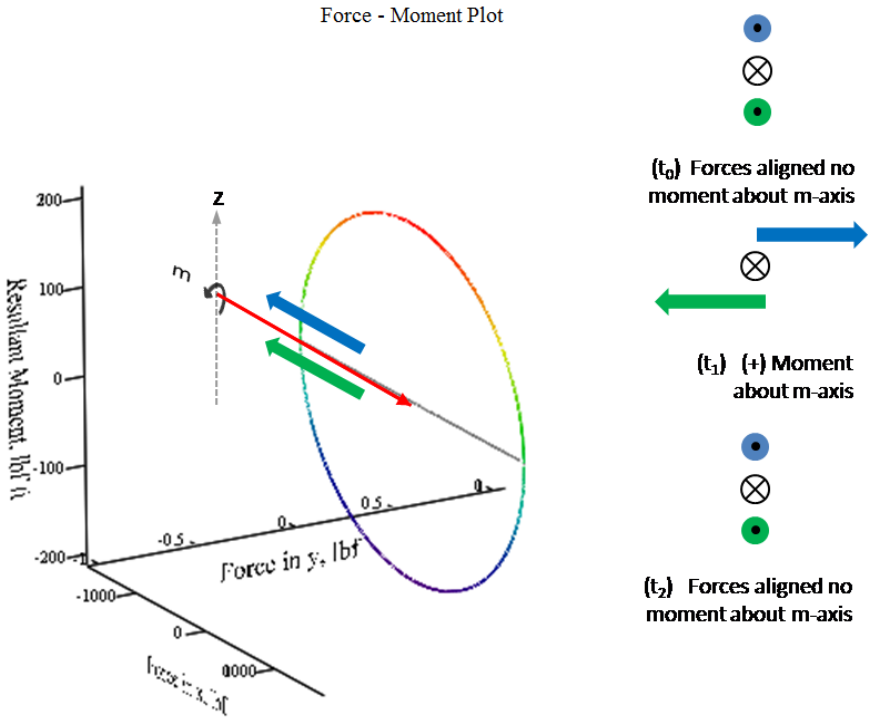

Figure 28. Force and Moment, at time t_2t_2

4. Time, t_3, again the moment is at a maximum (Figure 29). However, the direction of the moment has been reversed and is now negative relative to the m-axis. The moment directional change relative to the m-axis occurs every time the force vectors of the energy-wheels cross, creating a force maximum.

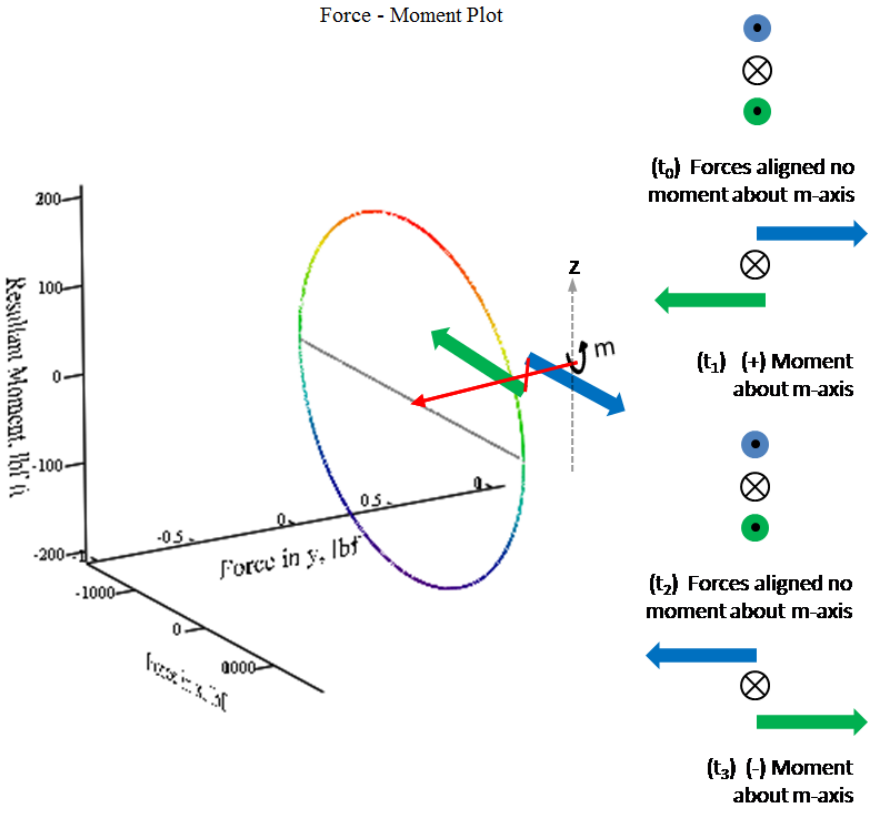

Figure 29. Force and Moment, at time t_3

A more advanced energy-wheel pattern having four force maximums is plotted in Figure 30, below. As is clearly seen at point **A,** the planer maximum is aligned with the moment minimum, and point **B** aligns the moment maximum with the force minimum. The direction of the moment changes with each crossing of the force maximum, point A.

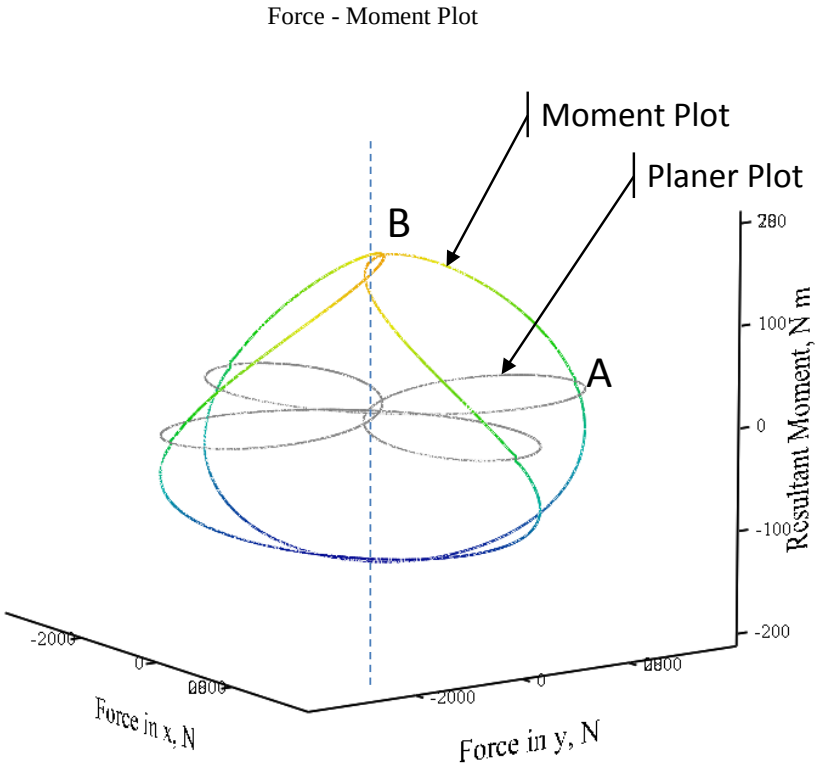

Figure 30. Moment magnitude and direction using local reference frame.

Returning to the modified star where there is a residual moment is due to the mass, vertical lever arm distance, and the angular velocity of the energy-wheels being different (Figure 31). Starting at a force maximum at A (Figure 31), the moment plot moves to a positive maximum moment about m-axis at B, then goes back to a moment minimum/force maximum at C. At C, the planer force maximum, there still exists a residual moment created by the mass, mass center, and angular velocity differences between the two energy-wheels. At this instantaneous point C, the resulting moment magnitude is about the n-axis. At the next time increment, the direction of the moment about the m-axis changes sign. The moment goes to the next moment maximum D, and another minimum E. The magnitude of this residue moment in the sample plot is approximately 100 N m

Force - Moment Plot

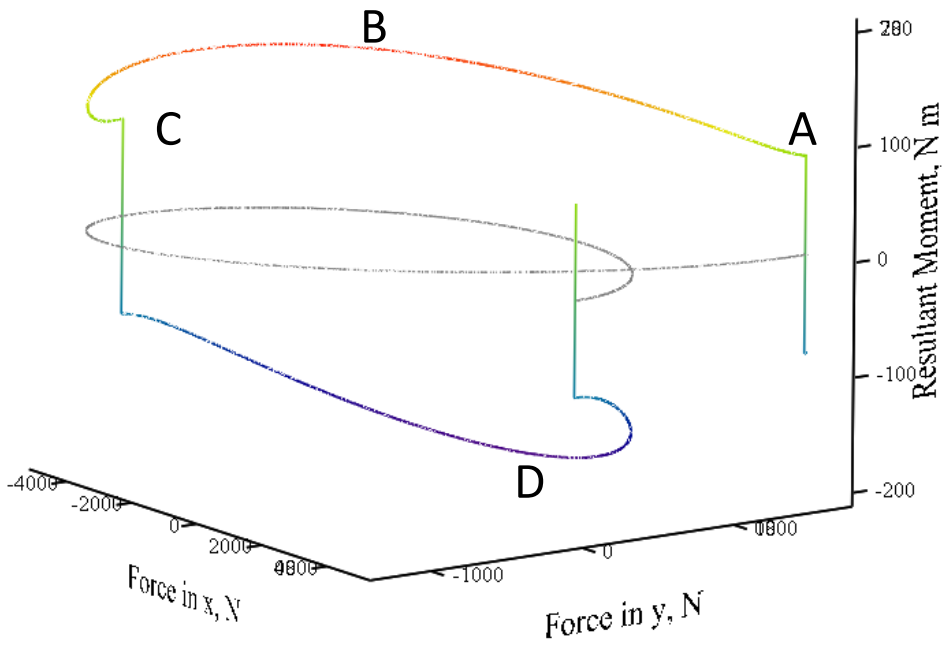

Figure 31. Peak to peak with negative moment

SYSTEM EFFICIENCY

With discussion of the force and moments complete, the following analysis focussed on the system efficiency of transferring useful forces to the tree, using a simplified model developed with the following assumptions:

1. All x-axis forces are transferable to the tree trunk.
2. No y and z-axis forces are transferred.
3. No moment forces transfer. Moments are diffused or cancelled by the pads, slings, sling lubrication, and the suspending structure.

By idealizing the slings and pad system to a non-form fitting system and establishing the coefficient of friction between the slings as zero, then the only forces the shaker can transfer to the tree are normal to the sling friction surface. Due to the absence of friction, all moments and the y and z-axis would be allowed to slip until resisting forces from the frame and hanger balanced the system.

The modified star has the same interaction of moments and forces as the simplified bidirectional linear model. The difference is the modified star pattern requires the energy-wheels have different mass, angular velocity, and center of gravity locations, which causes there to be both residue moments and forces. This is represented by the fact that neither the force or the moment ever have a zero value, shown in Figure 32.

The three-dimensional plot has a shadow plot in the (x-y) plane of Figure 33 to provide visual reference to the previously discussed planer shaker-head pattern and the corresponding moment magnitude. The magnitude of the moment is normalized to better illustrate the relationship between plane forces. The energy-wheel moments cause the shaker head to roll, tilt, or pivot relative to the tree trunk and the reaction forces of the transportation system. The reactions at the trunk must be dissipated by the slings lubrication as torsion and sliding, or the bark can be damaging. The moments

generated by stacked rotating mass energy-wheels are non-normal forces and represent a significant consumption of energy. In addition to the slings and pads dissipating energy, the shaker head transporter must also dissipate reaction forces of the moments resulting in friction, heat, and structural strain.

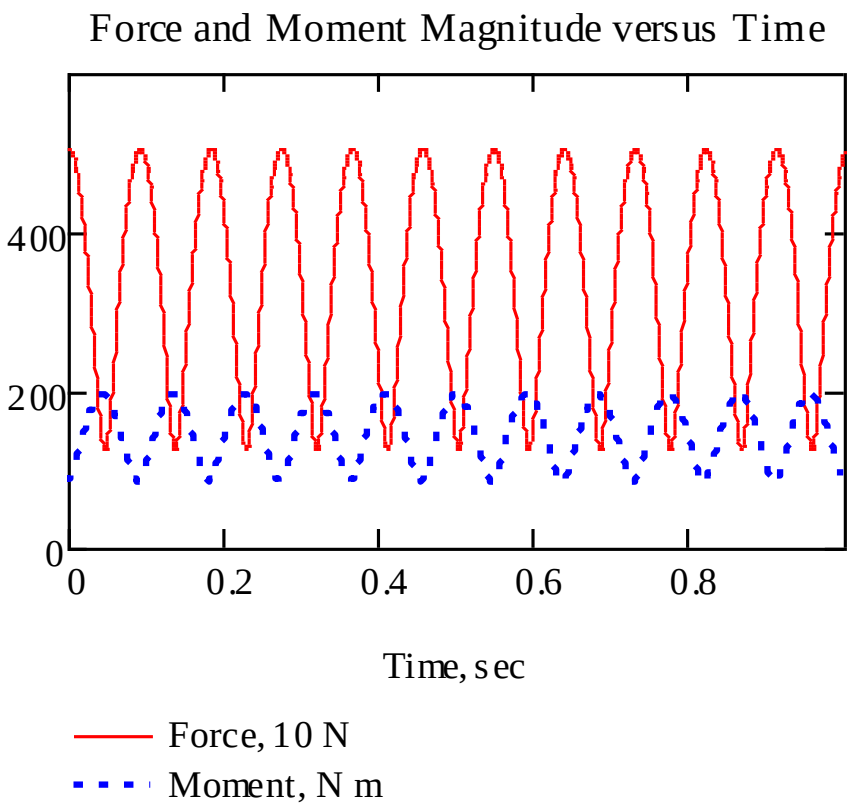

Figure 32. Planer plot of moment and force magnitude for the modified star shaker pattern, 100% y-axis displacement efficiency.

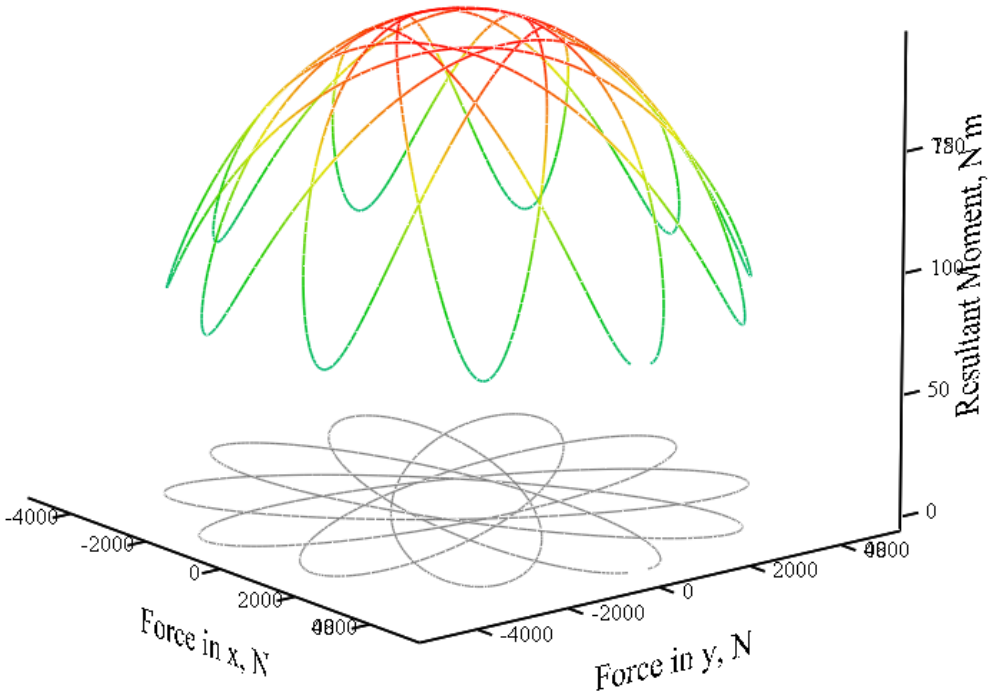

Figure 33. Plot of moment and force magnitude for the modified star shaker pattern, 100% y-axis displacement efficiency.

Abdel-Fattah (2003) found the efficiency of the slings and pads to transmit non-normal displacement to the tree trunk in the y-axis averaged 66%. The deflection of the tree is proportional to the forces if modulus of elasticity and diameter are constant, and the trunk is assumed rigidly mounted cantilevered beam. Using this information on the modified star pattern an efficiency variable (η_y) is applied to the stacked eccentric mass energy-wheel system model and set to 66%. The loss of force transfer in the y-axis is visible in both Figure 34 and Figure 35.

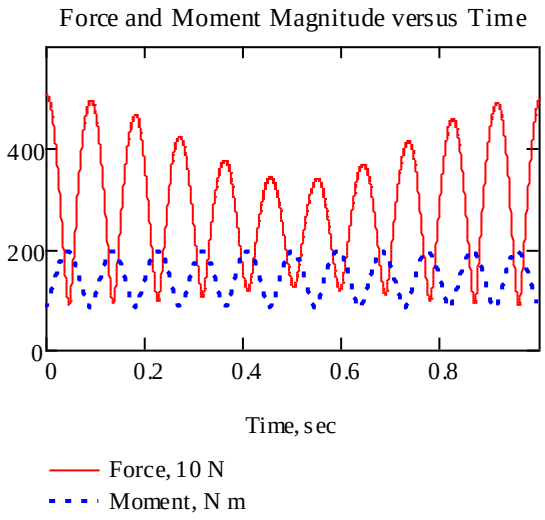

Figure 34. Planer plot of moment and force magnitude for the modified star shaker pattern, 66% y-axis displacement efficiency.

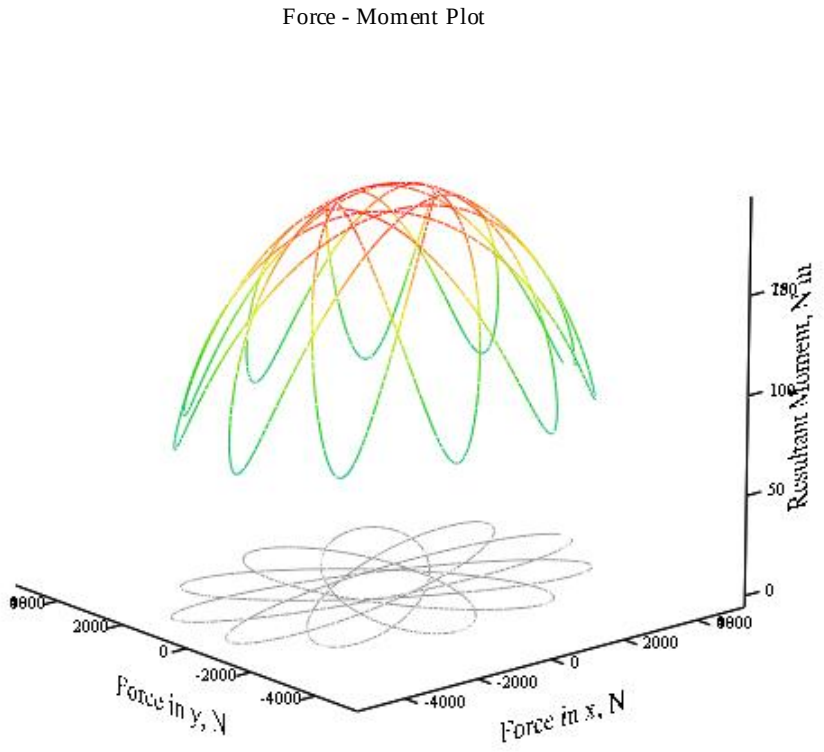

Figure 35. Plot of moment and force magnitude for the modified star shaker pattern, 66% y-axis displacement efficiency.

DISCUSSION OF FINDINGS

The plot of the Modified Star shown in Figure 36 highlights the complexity of the force and moments that a stacked eccentric mass counter rotating energy-wheel system creates; a historical planer model is plotted in light grey on (x-y) plane. The vertical line that is at each force maximum is only a connector line due to plotting and represents a residual moment.

The force magnitude plots show the stacked counter rotating eccentric mass energy-wheel system is not planer and simple, but is a complex and dynamic system; and for decades, machine builders have applied significant resources toward mitigating the symptoms of rotating mass energy-

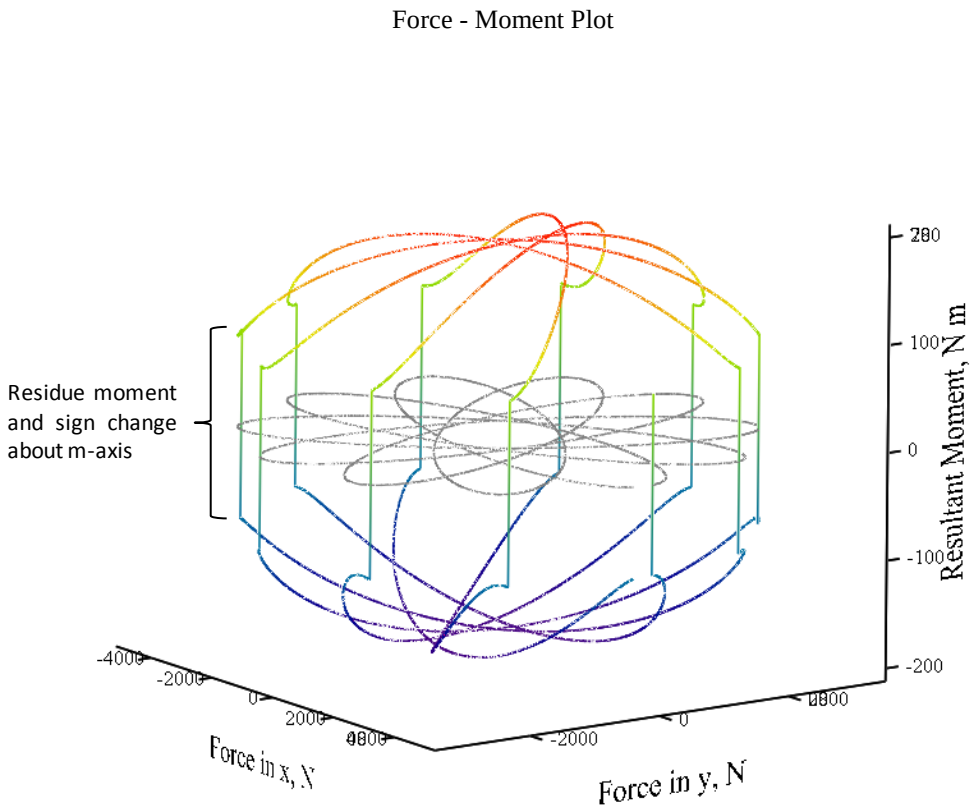

Figure 36. Modified Star, 66.% y-axis efficiency, moment magnitude, and direction

wheels without knowledge of the true dynamics of the system, i.e. the moments. Therefore, proposed solutions to tree damage and equipment failure were based on presumptions. An example of such a solution is the installation of a free sliding mass at the rear of the shaker head claiming to be a force generator (Figure 37). Matthews (1991) claimed it solved the cause of damaging forces:

> This invention; a mass mounted upon a tree shaking device in such a manner so that the forces generated by the weight alignment are either blocked or regenerated as force back to the tree. This invention solves the problem of rotational forces pivoting about the tree. The attempts to solve this problem have heretofore been dealing with the affect. This invention eliminates the cause. (p 1, line 61-68)

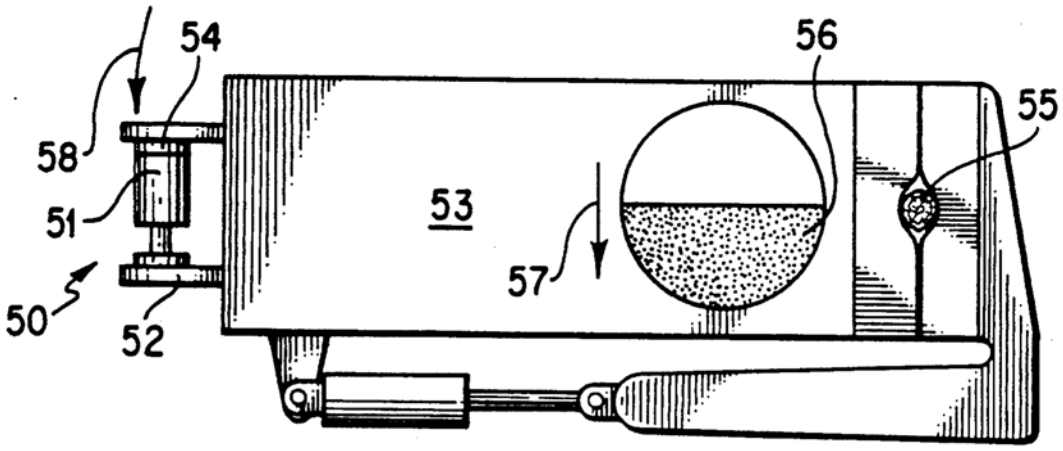

Figure 37. Tree shaker force regenerator

Recent trends toward timing the energy-wheels on the same plane using the planer model assumptions, will still result in the moments causing damage and requiring additional hardware and increased transportation structure size to dissipate or absorb the energy. With a system of planer eccentric masses there will be a reduction in moments about the x and y-axis; on the other hand, moment about a z-axis could cause excessive rotation about the tree trunk, causing barking. The displacement about a z-axis will again require the constraining of the system by the carrier structure

to prevent the moment from occurring around the tree or mechanical systems to dissipate the non-normal forces. This again would drive the physical size of the transportation system larger.

More analysis is required to determine if the vertical displacement discovered by Abdel-Fattah (2003) effects a maximum positive moment about the x-axis (Figure 12). This would make sense, since when the moment's maximum is about the x-axis; the rear hangers see a tension force and the two front hangers see a compressive force. The front hangers under compressive force slide off axis, collapsing, and allowing a vertical displacement of the shaker head. Since there are no planer forces that could apply a vertical lifting of the tree, moments could be a very viable explanation to this movement.

In the presented models, the x-axis forces are assumed 100% transferred and the y-axis force is assumed at 66% transferred into displacement. After the tree has been displaced, and the forces vector diminishes to a value less than the tree restitution forces, the tree will become the driver and the forces applied in the x-y axis may not contribute to the shaking energy and represent additional losses. The pads and slings again would dissipate non-normal forces further reducing the overall efficiency of energy transfer to the tree.

There are significant problems related to the current mechanized tree harvesting systems regarding tree damage; however, the cost of stopping mechanical harvesting is too great. As long as rotational energy is the basic system for tree stimulation, there will be unwanted forces that need to be dissipated or constrained. Without a systematic analysis of the customer requirements, tree response, and hardware optimization, the deficiencies of the system will continue.

CONCLUSIONS

First, the resulting forces of a stacked counter rotating eccentric mass energy-wheel system are not simply planer. The moments generated by the energy-wheel system are significant in magnitude and are non-value added. Moments will exist in any vibration system using rotating eccentric masses weight in a stacked or planer orientation. With the existence of moment energy dissipating systems such as the slings, pad, and suspension systems will be required to minimize the potential for tree damage. The continued belief that the system is planer will not inspire engineered solutions reducing tree damage, improving system efficiency, or increasing the diversity of application of mechanical tree harvesting.

Second, moments (M_x, M_y, and M_z) and forces (F_x, F_y, and F_z) do not and cannot be negated in a typical stacked counter rotating energy-wheel system by mechanical timing. There are always residue moments at the planer force maxima and residue forces at the moment maxima, except in special simplified cases.

Third, moments are possibly the most damaging force to the biological structure of tree trunks. Without proper sling lubrication, moments are possibly the largest contributing force to barking and vertical tree displacement. Engineering solutions that minimize or eliminate moments should increase the productive life of an orchard, minimize individual tree damage, reduce harvest cost, and reduce stress related to the cultural requirement of mechanical tree harvesting.

FUTURE RESEARCH

1. Tree shaker and trunk response analysis at the clamp zone using a three-dimensional driver model.
2. Analysis of the moments of tree shaker head and the displacement of the tree trunk.
3. Repeat the Abedel-Fattah (2003) research and recored the energy wheel speed, hyraulic motor oil pressure, and add six axis accellerometers to calculate the system efficiency.

ACKNOWLEDGEMENT

A special thanks to Teresa A. Snell, my wife for patiently supporting me throughout ten years of late nights, early mornings, and the untold cost for classes, computer hardware, software, data collection systems, travel expenses, and other incurred academic expenses. We are beginning to complete a long and special journey.

To Dr. Stuart Birrell, for having the vision to see the potential of this research and creating opportunities to rekindle my dream of engineering a better tree shaker.

REFERENCES

Abedel-Fattah, H. S. (2003). Substantial Vertical Tree Displacements During Almond Shaker Harvesting. *Applied Engineering in Agriculture* , Vol19(2) 145-150.

Almond Board of California. (2007). 2007 Almond Almanac, Document #5260.

Almond Board of California. (2008). *Almond Board*. Retrieved July 17, 2008, from Life cycle of almonds: http://www.almondboard.com/content/eLearning/lifecycle_of_almond_course/htmls/main.htm

Bell, J. (2001, Autumn). *American Forests.* Retrieved July 19, 2008, from The Tasty Pecan: http://www.americanforests.org/productsandpubs/magazine/archives/2001autumn/inprofile.php

Blue Diamond Growers. (2008). *Blue Diamond.* Retrieved May 6, 2008, from Growers: http://www.bluediamond.com/growers/techniques/cultural/all_shook_up.cfm

Chiel, D., & Zehavi, E. (1998). *Patent No. 5,816,037.* Afula Ilit, IL.

Clarence E. Hood, J., Alper, Y., & Webb, B. K. (1979). *Patent No. 4,170,100.* Clemson, S.C.

Compton, I. (1990). *Patent No. 4,921,073.* Chico, CA.

Compton, I. (1990b). *Patent No. 4,921,073.* Chico, CA.

Compton, I. (1990a). *Patent No. 4,932,195.* Chico, CA.

Compton, I. (1995). *Patent No. 5,467,588.* Chico, CA.

Davis, D. (2008, June). Manager, Alina Farms, McFarland, CA. (L. Snell, Interviewer)

Ferrari, T. E., & Evans, D. (2002). *Patent No. 6,474,055.* Bakersfield, CA.

Freeman, M. W., Viveros, M. A., Klonsky, K. M., & De Moura, R. L. (2008). Sample cost to establish an almond orchard and produce almonds. *University of California Cooperative Extension* , 20.

Herrera, E. (2000, May). *Historical Background of Pecan Plantings in the Western Region.* Retrieved July 22, 2008, from http://www.cahe.nmsu.edu/pubs/_h/h-626.html

Hill, D. G. (1997). *Patent No. 5,563,097.* Yakima, WA.

Mattews, C. D. (1991). *Patent No. 4,998,402.* Sutter, CA.

Mayo, D. P. (2002). *Patent No. 6,658,834.* Yuba City, CA.

McConnell, J. L., & Edwards, J. L. (1990). New Techniques for Tree Shaking of Older Seed Orchards. *Tree Planters' Notes* , 26-28.

McCrill, K. L. (1992). *Patent No. 5,103,625.* Sutter, CA.

Michelson, Y. (1998). *Patent No. 5,765,349.* 37000 Pardes Hanna, IL.

Moser Fruit Tree Sales, Inc. (n.d.). *The New Fruit Grower.* Retrieved July 19, 2008, from Training systems: http://www.thenewfruitgrower.com/training_systems.htm

Mosz, N. (2002, Jan 14). *Pistachio Timeline.* Retrieved July 19, 2008, from http://pestdata.ncsu.edu/cropTimelines/pdf/CApistachio.pdf

Orchard Machinery Corporation. (2007). Sales brochure. 2700 Colusa Highway, Yuba City, CA 95993.

Reynolds, S. d., Domingos, P., Vieira, C. d., & Pedro, J. (1997). *Patent No. 5,595,054.*

Savage, B. W. (1981). *Patent No. 4,275,548.* Madill, OK.

Srivastava, A. K., Goering, C. E., & Rohrbach, R. P. (1996). *Engineering Principles of Agricultural Machines.* (P. DeVore-Hansen, Ed.) St. Joseph: American Society of Agricultural Engineers.

Stout, B. A. (1999). *CIGR Handbook of Agricultural Engineering, Vol. III Plant Production Engineering.* American Society of Agricultural Engineers.

United State Department of Agriculture. (2007). *Noncitrus Fruits and Nuts 2007 Summary.* National Agricultrual Statistic Service.

US Department of Agriculture, Forest Service, Forest Products Laboratory. (1999). Mechanical Properties of Wood. In D. W. Green, J. E. Winandy, & D. E. Krestschmann, *Wood book - Wood as an engineering material* (pp. Chapeter 4, p.4-8). Madison, WI.

Walnut Marketing Board. (2008, May). *Walnuts, Commodity Fact Sheet.* Retrieved July 19, 2008, from http://www.cfaitc.org/Commodity/pdf/Walnuts.pdf

Westerguard, R. (1983). *Patent No. 4409782.* Ceres, CA.

Zehavi, E., & Chiel, D. (1995). *Patent No. 5,473,875.* Kiriat Tivon 36000, IL.

Zehavi, E., & Chiel, D. (2005). *Patent No. 6,978,591.* Kiryat Tivon, IL.

APPENDIX A. STAR PLOTS THEORETICAL VS. 66% Y-AXIS EFFICIENCY

(US units)

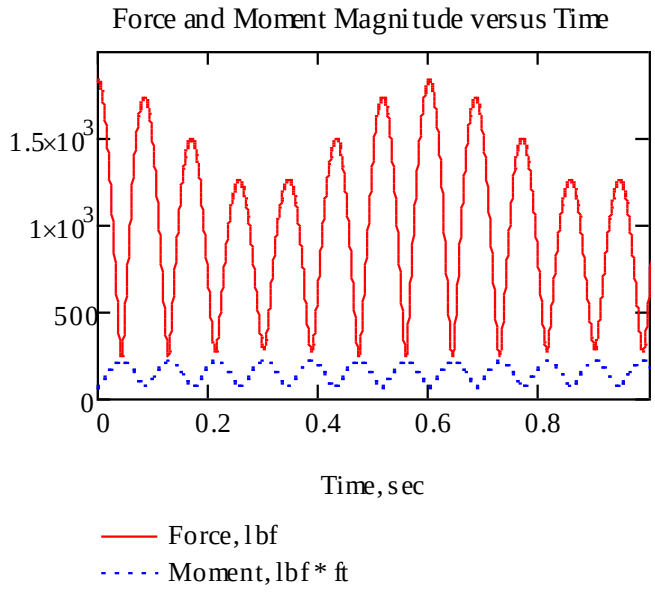

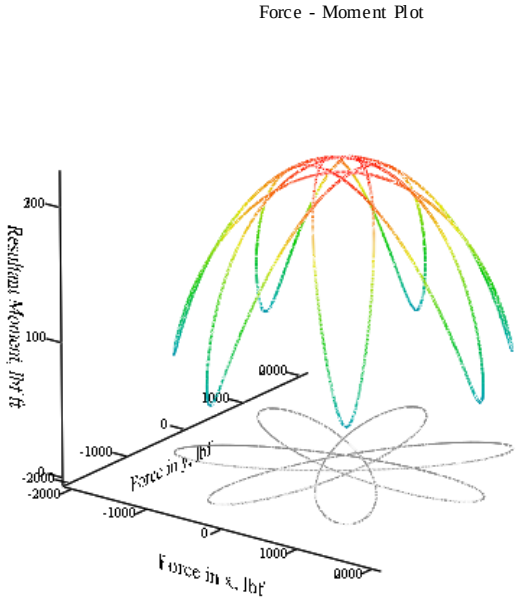

APPENDIX B. THINNING PLOTS THEORETICAL VS. 66% Y-AXIS EFFICIENCY

(US units)

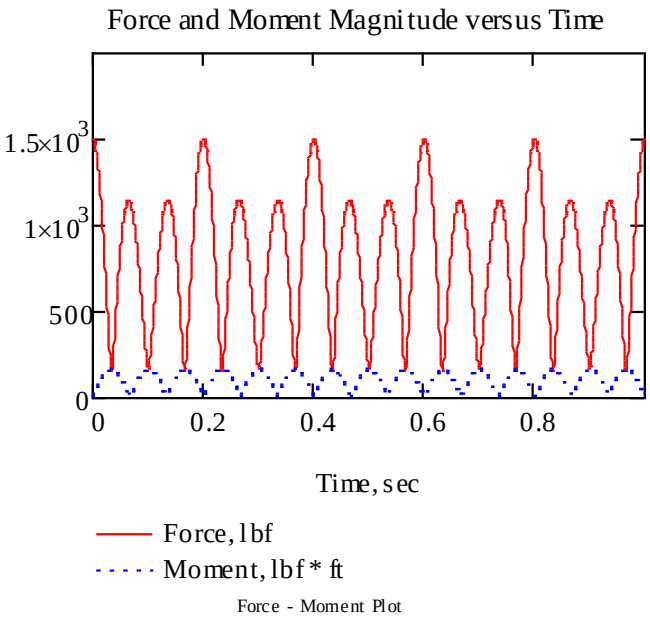

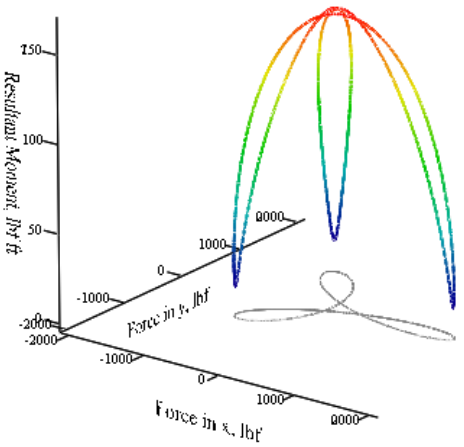

APPENDIX C. SPIRAL ORBIT PLOTS THEORETICAL VS. 66% Y-AXIS EFFICIENCY

(US Units)

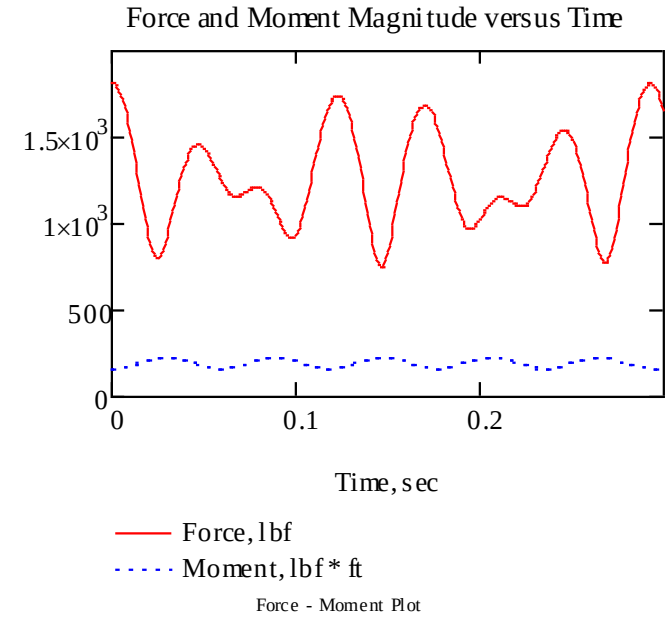

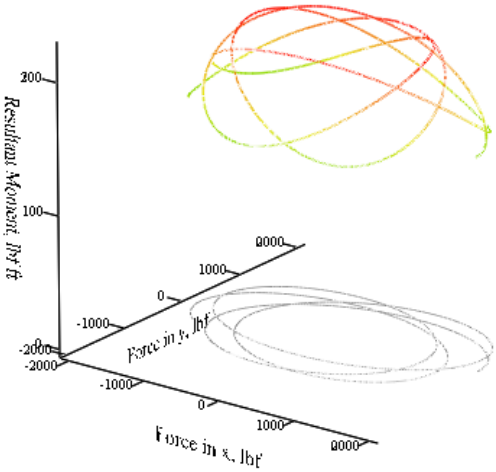

APPENDIX D. TRIANGLE PLOTS THEORETICAL VS. 66% Y-AXIS EFFICIENCY

(US Units)

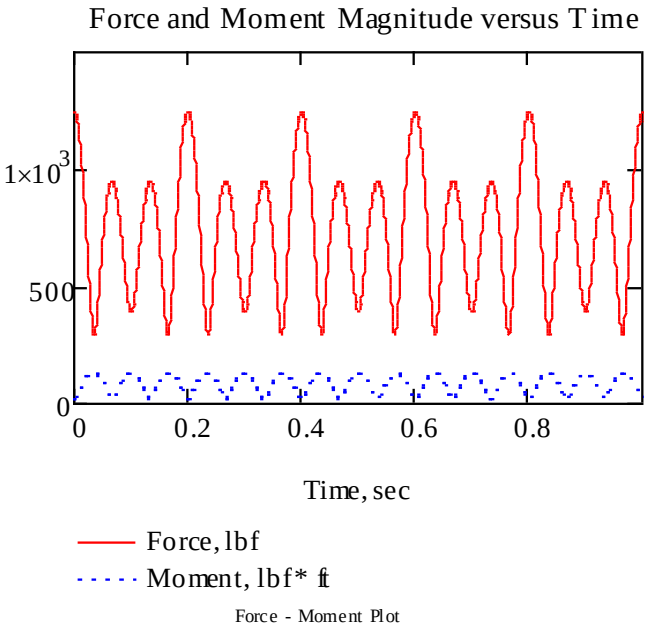

Force - Moment Plot

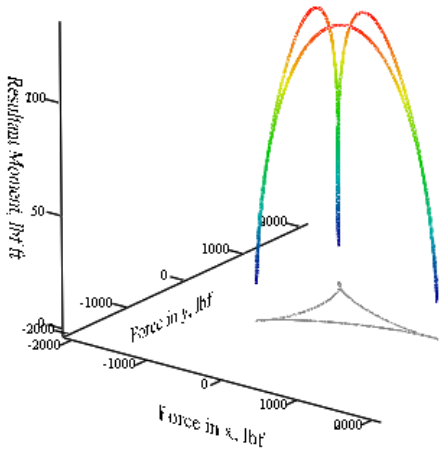

APPENDIX E. CRYSTAL BALL SAMPLE CODE FOR TREE 1 AND 2

Damage logic

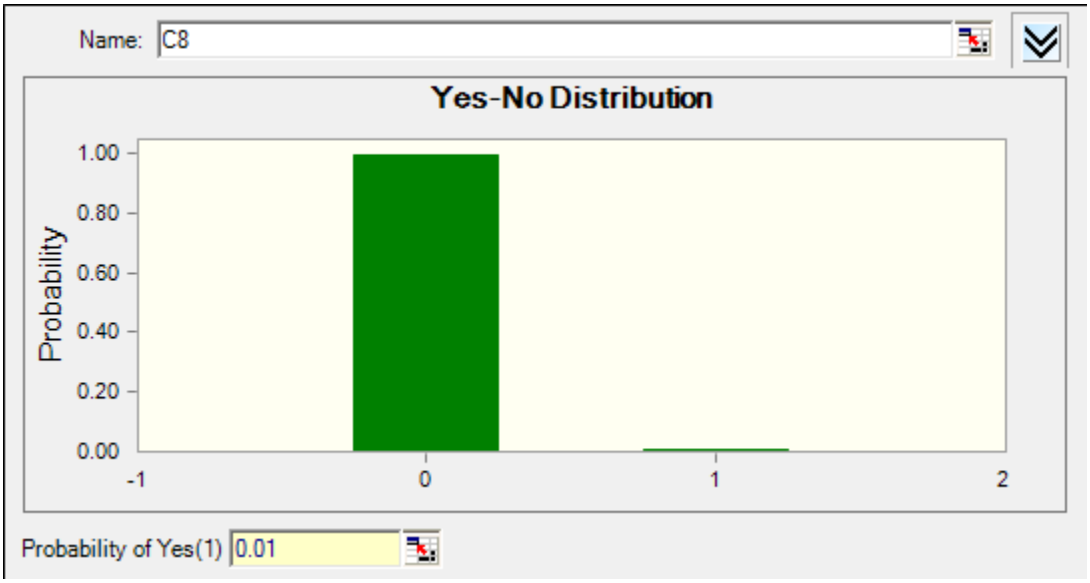

Gross harvest distribution

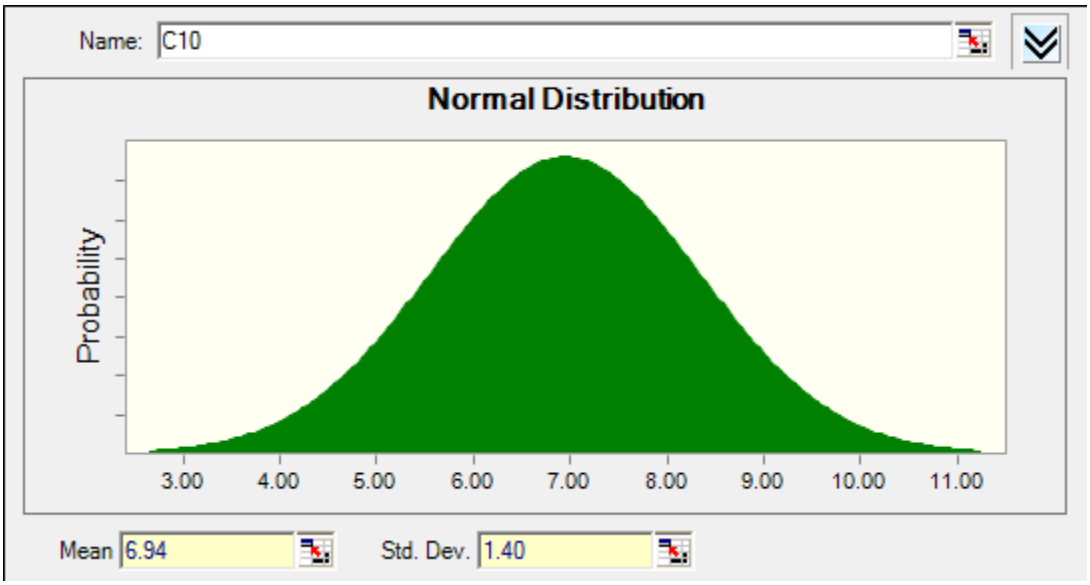

Code

Damage %	0.01		
Prod. / Tree	=Sheet2!C 15		
StDev / Tree	=Sheet2!C 16		

Acres, hectare	1	=C9+C15+C21+C27+C33+C39+C45+C51+C57+C63+C69+C75+C81+C87+C93+C99+C105+C111+C117+C123+C129	=D9+D15+D21+D27+D33+D39+D45+D51+D57+D63+D69+D75+D81+D87+D93+D99+D105+D111+D117+D123+D129
Tree Number		1	=C6+1
Age	5	5	5
Damage Logic		0	0
Harvest Logic		=IF(C7>=5,1,0)	=IF(D7>=5,1,0)
Gross Harvest		0	0
Net Harvest		=C10*C9	=D10*D9
Age	=B7+1	=IF(AND(C8=1,C7>=5),0,C7+1)	=IF(AND(D8=1,D7>=5),0,D7+1)
Damage Logic		0	0
Harvest Logic		=IF(C13>=5,1,0)	=IF(D13>=5,1,0)
Gross Harvest		0	0
Net Harvest		=C16*C15	=D16*D15
Age	=B13+1	=IF(AND(C14=1,C13>=5),0,C13+1)	=IF(AND(D14=1,D13>=5),0,D13+1)
Damage Logic		0	0
Harvest Logic		=IF(C19>=5,1,0)	=IF(D19>=5,1,0)
Gross Harvest		0	0
Net Harvest		=C22*C21	=D22*D21
Age	=B19+1	=IF(AND(C20=1,C19>=5),0,C19+1)	=IF(AND(D20=1,D19>=5),0,D19+1)
Damage Logic		0	0
Harvest Logic		=IF(C25>=5,1,0)	=IF(D25>=5,1,0)
Gross Harvest		0	0
Net Harvest		=C28*C27	=D28*D27
Age	=B25+1	=IF(AND(C26=1,C25>=5),0,C25+1)	=IF(AND(D26=1,D25>=5),0,D25+1)
Damage Logic		0	0
Harvest Logic		=IF(C31>=5,1,0)	=IF(D31>=5,1,0)
Gross Harvest		0	0
Net Harvest		=C34*C33	=D34*D33
Age	=B31+1	=IF(AND(C32=1,C31>=5),0,C31+1)	=IF(AND(D32=1,D31>=5),0,D31+1)
Damage Logic		0	0
Harvest Logic		=IF(C37>=5,1,0)	=IF(D37>=5,1,0)
Gross Harvest		0	0
Net Harvest		=C40*C39	=D40*D39
Age	=B37+1	=IF(AND(C38=1,C37>=5),0,C37+1)	=IF(AND(D38=1,D37>=5),0,D37+1)

Damage Logic		0	0
Harvest Logic		=IF(C43>=5,1,0)	=IF(D43>=5,1,0)
Gross Harvest		0	0
Net Harvest		=C46*C45	=D46*D45
Age	=B43+1	=IF(AND(C44=1,C43>=5),0,C43+1)	=IF(AND(D44=1,D43>=5),0,D43+1)
Damage Logic		0	0
Harvest Logic		=IF(C49>=5,1,0)	=IF(D49>=5,1,0)
Gross Harvest		0	0
Net Harvest		=C52*C51	=D52*D51
Age	=B49+1	=IF(AND(C50=1,C49>=5),0,C49+1)	=IF(AND(D50=1,D49>=5),0,D49+1)
Damage Logic		0	0
Harvest Logic		=IF(C55>=5,1,0)	=IF(D55>=5,1,0)
Gross Harvest		0	0
Net Harvest		=C58*C57	=D58*D57
Age	=B55+1	=IF(AND(C56=1,C55>=5),0,C55+1)	=IF(AND(D56=1,D55>=5),0,D55+1)
Damage Logic		0	0
Harvest Logic		=IF(C61>=5,1,0)	=IF(D61>=5,1,0)
Gross Harvest		0	0
Net Harvest		=C64*C63	=D64*D63
Age	=B61+1	=IF(AND(C62=1,C61>=5),0,C61+1)	=IF(AND(D62=1,D61>=5),0,D61+1)
Damage Logic		0	0
Harvest Logic		=IF(C67>=5,1,0)	=IF(D67>=5,1,0)
Gross Harvest		0	0
Net Harvest		=C70*C69	=D70*D69
Age	=B67+1	=IF(AND(C68=1,C67>=5),0,C67+1)	=IF(AND(D68=1,D67>=5),0,D67+1)
Damage Logic		0	0
Harvest Logic		=IF(C73>=5,1,0)	=IF(D73>=5,1,0)
Gross Harvest		0	0
Net Harvest		=C76*C75	=D76*D75
Age	=B73+1	=IF(AND(C74=1,C73>=5),0,C73+1)	=IF(AND(D74=1,D73>=5),0,D73+1)
Damage Logic		0	0
Harvest Logic		=IF(C79>=5,1,0)	=IF(D79>=5,1,0)
Gross Harvest		0	0
Net Harvest		=C82*C81	=D82*D81
Age	=B79+1	=IF(AND(C80=1,C79>=5),0,C79+1)	=IF(AND(D80=1,D79>=5),0,D79+1)

Damage Logic		0	0
Harvest Logic		=IF(C85>=5,1,0)	=IF(D85>=5,1,0)
Gross Harvest		0	0
Net Harvest		=C88*C87	=D88*D87
Age	=B85+1	=IF(AND(C86=1,C85>=5),0,C85+1)	=IF(AND(D86=1,D85>=5),0,D85+1)
Damage Logic		0	0
Harvest Logic		=IF(C91>=5,1,0)	=IF(D91>=5,1,0)
Gross Harvest		0	0
Net Harvest		=C94*C93	=D94*D93
Age	=B91+1	=IF(AND(C92=1,C91>=5),0,C91+1)	=IF(AND(D92=1,D91>=5),0,D91+1)
Damage Logic		0	0
Harvest Logic		=IF(C97>=5,1,0)	=IF(D97>=5,1,0)
Gross Harvest		0	0
Net Harvest		=C100*C99	=D100*D99
Age	=B97+1	=IF(AND(C98=1,C97>=5),0,C97+1)	=IF(AND(D98=1,D97>=5),0,D97+1)
Damage Logic		0	0
Harvest Logic		=IF(C103>=5,1,0)	=IF(D103>=5,1,0)
Gross Harvest		0	0
Net Harvest		=C106*C105	=D106*D105
Age	=B103+1	=IF(AND(C104=1,C103>=5),0,C103+1)	=IF(AND(D104=1,D103>=5),0,D103+1)
Damage Logic		0	0
Harvest Logic		=IF(C109>=5,1,0)	=IF(D109>=5,1,0)
Gross Harvest		0	0
Net Harvest		=C112*C111	=D112*D111
Age	=B109+1	=IF(AND(C110=1,C109>=5),0,C109+1)	=IF(AND(D110=1,D109>=5),0,D109+1)
Damage Logic		0	0
Harvest Logic		=IF(C115>=5,1,0)	=IF(D115>=5,1,0)
Gross Harvest		0	0
Net Harvest		=C118*C117	=D118*D117
Age	=B115+1	=IF(AND(C116=1,C115>=5),0,C115+1)	=IF(AND(D116=1,D115>=5),0,D115+1)
Damage Logic		0	0
Harvest Logic		=IF(C121>=5,1,0)	=IF(D121>=5,1,0)
Gross Harvest		0	0
Net Harvest		=C124*C123	=D124*D123
Age	=B121+1	=IF(AND(C122=1,C121>=5),0,C121+1)	=IF(AND(D122=1,D121>=5),0,D121+1)

Damage Logic		0	0
Harvest Logic		=IF(C127>=5,1,0)	=IF(D127>=5,1,0)
Gross Harvest		0	0
Net Harvest		=C130*C129	=D130*D129
Age	=B127+1	=IF(AND(C128=1,C127>=5),0,C127+1)	=IF(AND(D128=1,D127>=5),0,D127+1)
Damage Logic		0	0
Harvest Logic		=IF(C133>=5,1,0)	=IF(D133>=5,1,0)
Gross Harvest		0	0
Net Harvest		=C136*C135	=D136*D135
Age	=B133+1	=IF(AND(C134=1,C133>=5),0,C133+1)	=IF(AND(D134=1,D133>=5),0,D133+1)
Damage Logic		0	0
Harvest Logic		=IF(C139>=5,1,0)	=IF(D139>=5,1,0)
Gross Harvest		0	0
Net Harvest		=C142*C141	=D142*D141
Age	=B139+1	=IF(AND(C140=1,C139>=5),0,C139+1)	=IF(AND(D140=1,D139>=5),0,D139+1)
Damage Logic		0	0
Harvest Logic		=IF(C145>=5,1,0)	=IF(D145>=5,1,0)
Gross Harvest		0	0
Net Harvest		=C148*C147	=D148*D147
Age	=B145+1	=IF(AND(C146=1,C145>=5),0,C145+1)	=IF(AND(D146=1,D145>=5),0,D145+1)
Damage Logic		0	0
Harvest Logic		=IF(C151>=5,1,0)	=IF(D151>=5,1,0)
Gross Harvest		0	0
Net Harvest		=C154*C153	=D154*D153
Age	=B151+1	=IF(AND(C152=1,C151>=5),0,C151+1)	=IF(AND(D152=1,D151>=5),0,D151+1)
Damage Logic		0	0
Harvest Logic		=IF(C157>=5,1,0)	=IF(D157>=5,1,0)
Gross Harvest		0	0
Net Harvest		=C160*C159	=D160*D159

Picture of Excel with 242 tree columns

Damage %	0.01						
Prod. / Tree	6.9						
StDev / Tree	1.4						
Acres	1	21	21	20yrs Prod. Gross Potential	20yrs Prod. With 1.0% Shaker Damage	Number of Trees in Production	Lifetime production loss, kg/hectare
				-	-		-
Tree Number		1	242				
Age	5	5	5				
Damage Logic		0	0				
Harvest Logic		1	1			242	
Gross Harvest		0	0	0			
Net Harvest		0	0		0		
Age	6	6	6				
Damage Logic		0	0				
Harvest Logic		1	1			242	
Gross Harvest		0	0	0			
Net Harvest		0	0		0		
Age	7	7	7				
Damage Logic		0	0				
Harvest Logic		1	1			242	
Gross Harvest		0	0	0			
Net Harvest		0	0		0		
Age	8	8	8				
Damage Logic		0	0				
Harvest Logic		1	1			242	
Gross Harvest		0	0	0			
Net Harvest		0	0		0		
Age	9	9	9				
Damage Logic		0	0				
Harvest Logic		1	1			242	
Gross Harvest		0	0	0			
Net Harvest		0	0		0		
Age	10	10	10				
Damage Logic		0	0				
Harvest Logic		1	1			242	
Gross Harvest		0	0	0			
Net Harvest		0	0		0		
Age	11	11	11				
Damage Logic		0	0				
Harvest Logic		1	1			242	
Gross Harvest		0	0	0			
Net Harvest		0	0		0		
Age	12	12	12				
Damage Logic		0	0				
Harvest Logic		1	1			242	
Gross Harvest		0	0	0			
Net Harvest		0	0		0		
Age	13	13	13				
Damage Logic		0	0				
Harvest Logic		1	1			242	
Gross Harvest		0	0	0			
Net Harvest		0	0		0		
Age	14	14	14				
Damage Logic		0	0				
Harvest Logic		1	1			242	
Gross Harvest		0	0	0			
Net Harvest		0	0		0		
Age	15	15	15				
Damage Logic		0	0				
Harvest Logic		1	1			242	
Gross Harvest		0	0	0			
Net Harvest		0	0		0		
Age	16	16	16				
Damage Logic		0	0				
Harvest Logic		1	1			242	
Gross Harvest		0	0	0			
Net Harvest		0	0		0		
Age	17	17	17				
Damage Logic		0	0				
Harvest Logic		1	1			242	
Gross Harvest		0	0	0			
Net Harvest		0	0		0		
Age	18	18	18				
Damage Logic		0	0				
Harvest Logic		1	1			242	
Gross Harvest		0	0	0			
Net Harvest		0	0		0		
Age	19	19	19				
Damage Logic		0	0				
Harvest Logic		1	1			242	
Gross Harvest		0	0	0			
Net Harvest		0	0		0		
Age	20	20	20				
Damage Logic		0	0				
Harvest Logic		1	1			242	
Gross Harvest		0	0	0			
Net Harvest		0	0		0		
Age	21	21	21				
Damage Logic		0	0				
Harvest Logic		1	1			242	
Gross Harvest		0	0	0			
Net Harvest		0	0		0		
Age	22	22	22				
Damage Logic		0	0				
Harvest Logic		1	1			242	
Gross Harvest		0	0	0			
Net Harvest		0	0		0		
Age	23	23	23				
Damage Logic		0	0				
Harvest Logic		1	1			242	
Gross Harvest		0	0	0			
Net Harvest		0	0		0		
Age	24	24	24				
Damage Logic		0	0				
Harvest Logic		1	1			242	
Gross Harvest		0	0	0			
Net Harvest		0	0		0		
Age	25	25	25				
Damage Logic		0	0				
Harvest Logic		1	1			242	
Gross Harvest		0	0	0			
Net Harvest		0	0		0		
Age	26	26	26				
Damage Logic		0	0				
Harvest Logic		1	1			242	
Gross Harvest		0	0	0			
Net Harvest		0	0		0		
Age	27	27	27				
Damage Logic		0	0				
Harvest Logic		1	1			242	
Gross Harvest		0	0	0			
Net Harvest		0	0		0		
Age	28	28	28				
Damage Logic		0	0				
Harvest Logic		1	1			242	
Gross Harvest		0	0	0			
Net Harvest		0	0		0		
Age	29	29	29				
Damage Logic		0	0				
Harvest Logic		1	1			242	
Gross Harvest		0	0	0			
Net Harvest		0	0		0		
Age	30	30	30				
Damage Logic		0	0				
Harvest Logic		1	1			242	
Gross Harvest		0	0	0			
Net Harvest		0	0		0		

[i]Oracle Crystal Ball (formerly Decisioneering, Inc.)
Version 7.3.1
7700 Technology Way
Denver, Colorado 80237 USA
Main number: +1.303.334.4000

[ii] Mathcad 14.0
Copyright © 2007 Parametric Technology Corporation
PTC Corporate Headquarters
140 Kendrick Street
Needham, MA 02494 USA
781.370.5000